NASA
Technical
Paper
3057
DOE/NASA/
20320-77

December 1990

Wind Turbine Acoustics

Harvey H. Hubbard
and Kevin P. Shepherd

Work performed for
U.S. Department of Energy
Wind/Hydro/Ocean Technologies Division
and
Solar Energy Research Institute
Solar Technology Information Program

NASA

NASA Technical Paper 3057
DOE/NASA/ 20320-77

1990

Wind Turbine Acoustics

Harvey H. Hubbard
Planning Research Corporation
Hampton, Virginia

Kevin P. Shepherd
Langley Research Center
Hampton, Virginia

Work performed for
U.S. Department of Energy
Wind/Hydro/Ocean Technologies Division
and
Solar Energy Research Institute
Solar Technology Information Program
under Interagency Agreement DE-AI01-76ET-20320

NASA
National Aeronautics and Space Administration
Office of Management
Scientific and Technical Information Division

The text of this report is planned to appear as a chapter in a forthcoming book entitled *Wind Turbine Technology*. This is a joint project of the U.S. Department of Energy and the American Society of Mechanical Engineers, in which the NASA Lewis Research Center is responsible for technical editing and management. Production of the final text is under the sponsorship and direction of DOE's Solar Technical Information Programs Office. Book publication will be by the ASME.

Wind Turbine Acoustics

Harvey H. Hubbard

NASA Langley Research Center
and Planning Research Corporation
Hampton, Virginia

and

Kevin P. Shepherd, Ph.D.

NASA Langley Research Center
Hampton, Virginia

Introduction

Wind turbine generators, ranging in size from a few kilowatts to several megawatts, are producing electricity both singly and in wind power stations that encompass hundreds of machines. Many installations are in uninhabited areas far from established residences, and therefore there are no apparent environmental impacts in terms of noise. There is, however, the potential for situations in which the radiated noise can be heard by residents of adjacent neighborhoods, particularly those neighborhoods with low ambient noise levels. A widely publicized incident of this nature occurred with the operation of the experimental MOD-1 2-MW wind turbine (described in detail in Kelley *et al.* [1985]). Significant factors relevant to the potential environmental impact of wind turbine noise are listed in Figure 7-1.

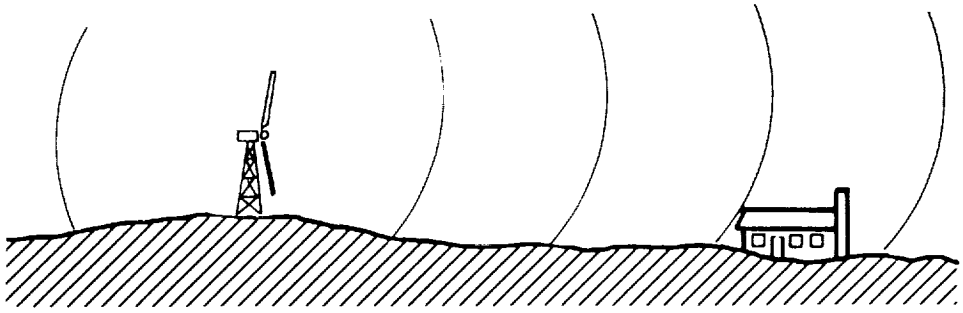

Figure 7-1. Factors contributing to wind turbine noise

The noise produced by wind turbines ranges in frequency from low values that are sometimes inaudible to higher values in the normal audible range [Kelley *et al.* 1985]. Although increased distance is beneficial in reducing noise levels, the wind can enhance noise propagation in certain directions and impede it in others. A unique feature of wind turbine noise is that it can result from essentially continuous periods of daytime and nighttime operation. This is in contrast to the more common aircraft and road traffic noises that vary markedly as a function of time of day.

This chapter summarizes available information on the physical characteristics of the noise generated by wind turbines and includes example sound pressure time histories, narrow-band and broadband frequency spectra, and noise radiation patterns. This chapter also reviews noise measurement standards, analysis technology, and a method for characterizing the noise from wind turbines. Prediction methods are summarized for both the low-frequency rotational harmonics and the broadband noise components caused by inflow turbulence, and also for turbulent boundary layers on the blades and wakes from the blade trailing edge. Also included are atmospheric propagation data that illustrate the effects of distance and the effects of refraction caused by a vertical gradient in mean wind speed for both upwind and downwind directions.

Perception thresholds for humans are defined for both narrow-band and broadband spectra from systematic tests in the laboratory and from observations in the field. Also summarized are structural vibrations and interior sound pressure levels, which could result from the low-frequency noise excitation of buildings.

A bibliography is available that lists technical papers on all aspects of wind turbine acoustics [Hubbard and Shepherd 1988].

Characteristics of Wind Turbine Noise

Noise from wind turbines may be categorized as aerodynamic or mechanical in origin. Aerodynamic noise components are either narrow-band (containing discrete harmonics) or broadband (random) and are related closely to the geometry of the rotor, its blades, and their aerodynamic flow environments. The low-frequency, narrow-band rotational components typically occur at the blade passage frequency (the rotational speed times the number of blades) and integer multiples of this frequency. Of lesser importance for most configurations are mechanical noise components from the operating bearings, gears, and accessories.

An example of a spectrum of wind turbine noise is shown in Figure 7-2. These data, which were measured 36 m downwind of a vertical-axis wind turbine (VAWT), show the decrease of sound pressure level with increasing frequency (a general characteristic of wind turbines). All sound pressure levels presented in this chapter are based on root-mean-square (RMS) values of pressure; they are referenced to 2×10^{-5} Pa and are averaged over 30 to 180 seconds, depending on the frequency bandwidth. The spectrum generally contains broadband random noise of aerodynamic origin, although discrete components identified as mechanical noise from the gearbox are also evident. The blade passage frequency is readily apparent in the time history illustrated in Figure 7-2, as is the random nature of the emitted sounds.

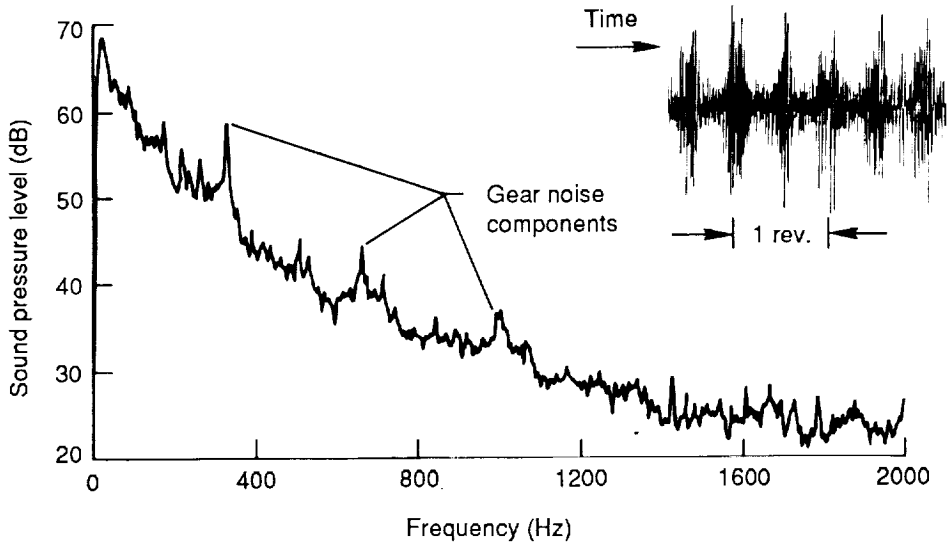

Figure 7-2. Typical narrow-band noise spectrum of a wind turbine, measured 36 m from a VAWT generating 185 kW at a wind speed of 16.5 m/s (bandwidth = 2.5 Hz)

The many analytical and experimental acoustical studies conducted on horizontal-axis wind turbines (HAWTs) indicate that for given geometrical and operational characteristics (such as power output, rotor area, and tip speed) HAWTs with downwind rotors will generate more noise than will those with upwind rotors. This is because an additional noise source in downwind rotors is introduced when the rotating blades interact with the aerodynamic wake of the supporting tower.

Because very little information on the acoustics of VAWTs is currently available, it is difficult to directly compare the noise-generation characteristics of HAWTs and VAWTs. Example VAWT spectra, levels, and directivity data are contained in Kelley, Hemphill, and Sengupta [1981] and Wehrey *et al.* [1987]. The blades of a VAWT interact with the aerodynamic wake of the rotor's central column in a manner similar to the way that a downwind HAWT rotor interacts with its tower wake, but at a greater distance relative to the column diameter. Thus, the magnitude of the noise from a VAWT caused by this interaction is expected to be less than that of an equivalent downwind HAWT rotor and greater than that of an upwind HAWT rotor. There is currently no detailed information available describing other aerodynamic noise sources associated with VAWTs. Thus, to gain an understanding of the acoustics of this type of turbine, additional studies are needed.

Blade Impulsive Noise

Impulsive noise is often associated with downwind rotors on HAWTs; in many cases, it is the dominant noise component for that configuration. Figures 7-3(a) and (b) show example sound pressure time histories for two different HAWTs with downwind rotors [Shepherd, Willshire, and Hubbard 1988; Hubbard and Shepherd 1982]. Figure 7-3(a) relates to a large-scale turbine with a 78.2-m-diameter rotor supported downwind of a twelve-sided shell tower. Strong impulses are superposed on less intense broadband components. The impulse noise arises from the blade's interaction with the aerodynamic wake of the tower. As each blade traverses the tower wake, it experiences short-duration load fluctuations caused by the velocity deficiency in the wake. These load fluctuations lead directly to the radiated acoustic pulses. The acoustic pulses are all of short duration and vary in amplitude as a function of time. This variation in amplitude is believed to result from variations in the blade loadings caused by detailed differences in the time-varying structure of the aerodynamic wake [Kelley *et al.* 1985].

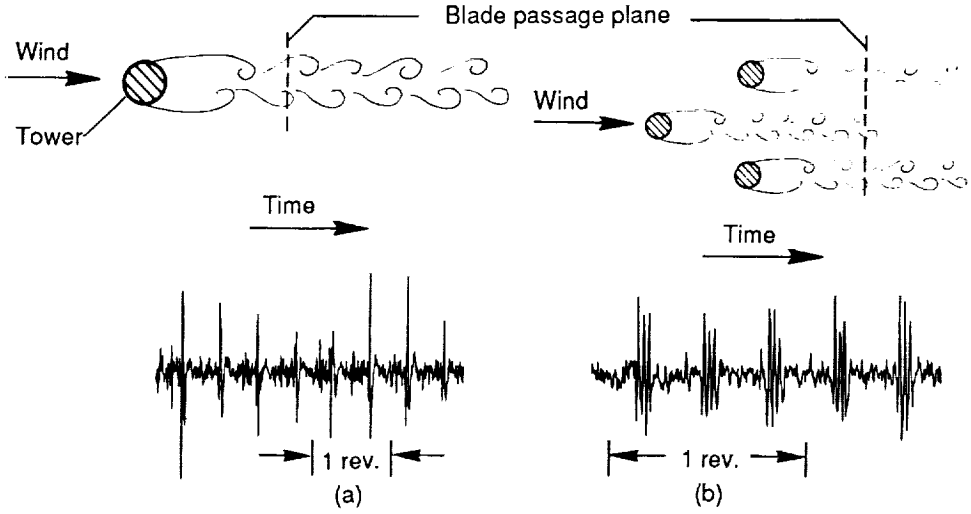

Figure 7-3. Sound pressure time histories from two downwind-rotor HAWTS [Shepherd, Willshire, and Hubbard 1988; Hubbard and Shepherd 1982]. (a) 78.2-m-diameter rotor, 2 blades, 2050-kW output, 30-rpm rotor speed, 200-m distance. (b) 17.6-m-diameter rotor, 3 blades, 5-kW output, 72-rpm rotor speed, 30.5-m distance.

The same phenomena, differing only in detail, are illustrated in Figure 7-3(b). These data relate to a small-scale turbine with a 17.6-m-diameter rotor supported downwind of a three-legged open truss tower [Hubbard and Shepherd 1982]. Each blade passage produces a three-peaked pulse as the blade interacts with the wakes of the three tower legs. Experimental studies by Hubbard and Shepherd [1982] and Greene [1981] showed that the character of the wake of a tower element can be altered to various degrees by adding such modifications as strakes, screens, and vanes. Because some velocity deficiency remains in the lee of the tower, it is inevitable that such modifications can ameliorate but not eliminate the impulsive noise components.

Figure 7-4 compares narrow-band spectra for upwind-rotor and downwind-rotor HAWTs along with their associated sound pressure time histories. The upwind rotor is 91 m in diameter and operates at a speed of 17.5 rpm. The downwind rotor is 78.2 m in diameter and rotates at 30 rpm. Note that the upwind-rotor spectrum shows an amplitude-modulated time history but without the sharp pressure peaks that are evident for the downwind rotor. Although the two spectra have essentially the same shapes, the

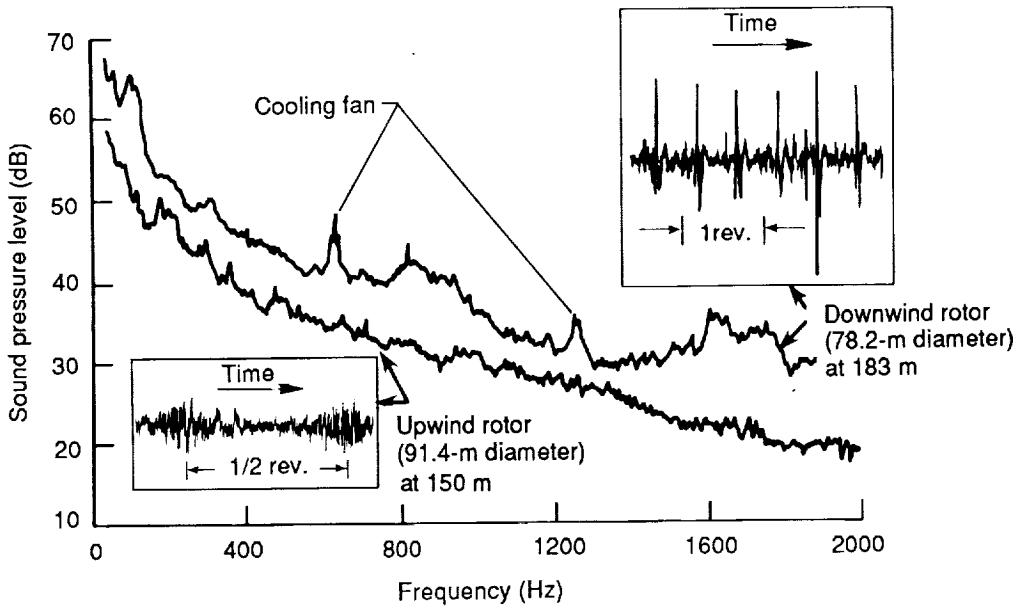

Figure 7-4. Narrow-band noise spectra from large-scale HAWTS with upwind and downwind rotors (bandwidth = 2.5 Hz)

downwind-rotor spectrum shows generally higher noise levels because of the downwind rotor's higher blade tip speed.

The lower-frequency portions of the spectra (Figure 7-4) were analyzed with a narrower effective bandwidth resolution, and an expanded frequency scale is shown in Figure 7-5. Impulsive noises such as those illustrated in Figures 7-3(a) and 7-4 can be

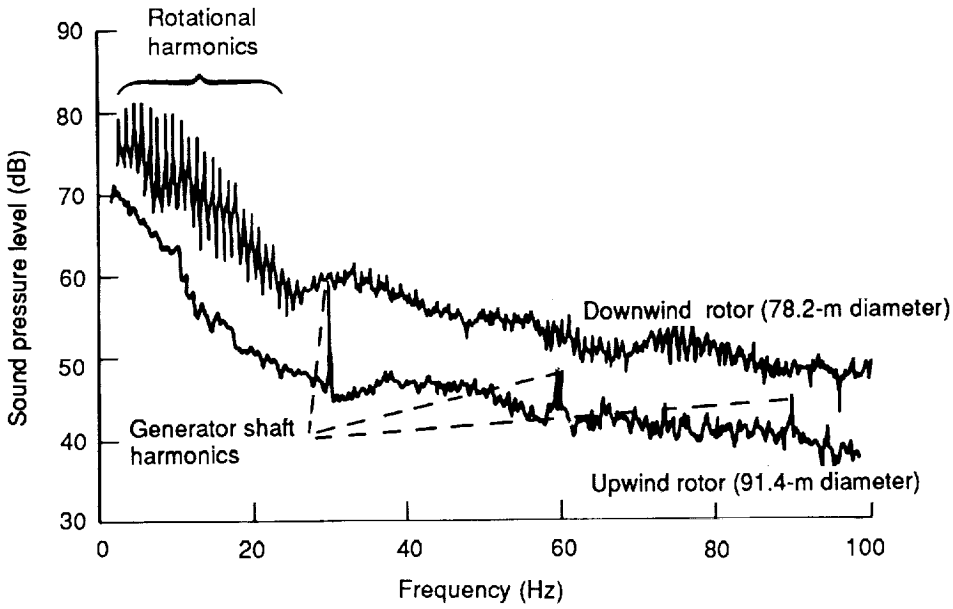

Figure 7-5. Low-frequency, narrow-band noise spectra from large-scale HAWTs with upwind and downwind rotors (bandwidth = 0.25 Hz, distance = 150 m)

resolved into their Fourier components, which are pure tones at the blade passage frequency and integer harmonics of this frequency. These components are evident in the low-frequency portion of the downwind-rotor spectrum of Figure 7-5, which shows identifiable rotational components out to about 30 Hz. The spectrum indicates a peak near 5 Hz and then a general decrease as the frequency increases [Shepherd and Hubbard 1983].

Figure 7-6 illustrates the nature of the noise radiation patterns for low-frequency rotational noise components. Shown are the results of simultaneous measurements of sound pressure levels at a frequency of 8 Hz; the measurements were taken at a distance of 200 m around the turbine. Acoustic radiations upwind and downwind are about equal and are greater than that in the crosswind direction. The two patterns in Figure 7-6 provide a direct comparison of measurements made at the same nominal wind conditions for daytime and nighttime operation. The nighttime levels are generally lower than the daytime levels, and the resulting radiation pattern generally appears as an acoustic dipole. The lower levels are believed to result from a different atmospheric turbulence structure during the night.

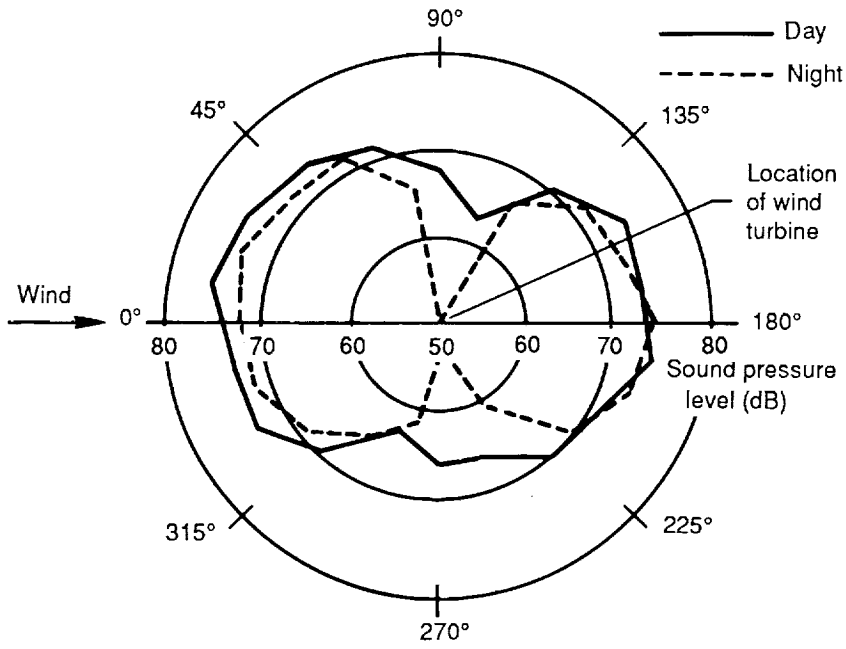

Figure 7-6. Example radiation patterns for low-frequency rotational noise 200 m from a large-scale HAWT (harmonic frequency = 8 Hz, wind speed = 7.2 m/s, power = 100 kW) [Shepherd, Willshire, and Hubbard 1988]

Kelley, Hemphill, and McKenna [1982] compare characteristic low-frequency noise emissions from upwind-rotor HAWTs, downwind-rotor HAWTs, and a VAWT. These comparisons are based on joint probability distributions of octave-band sound pressure levels. The authors conclude that a downwind-rotor HAWT presents the highest probability of emitting coherent low-frequency noise, although an upwind-rotor HAWT appears to have the lowest probability of emitting such noise. The probability associated with a VAWT providing coherent noise was found to be between the two HAWT probabilities.

Blade Broadband Noise

Broadband noise arises as the rotating blades interact with the wind inflow to the rotor. It is a significant component for all configurations of rotors, regardless of whether the low-frequency impulsive components are present. Broadband noise components are characterized by a continuous distribution of sound pressure with frequency and dominate a typical wind turbine acoustic spectrum at frequencies above about 100 Hz.

Example broadband-noise radiation patterns for a large-scale HAWT are shown in Figure 7-7. Data are included for one-third-octave bands with center frequencies of 100, 200, and 400 Hz. The band levels in the upwind and downwind directions are comparable but generally higher than those in the crosswind direction. The general shapes of these patterns are similar to those in Figure 7-6 for the low-frequency, rotational noise components during the daytime.

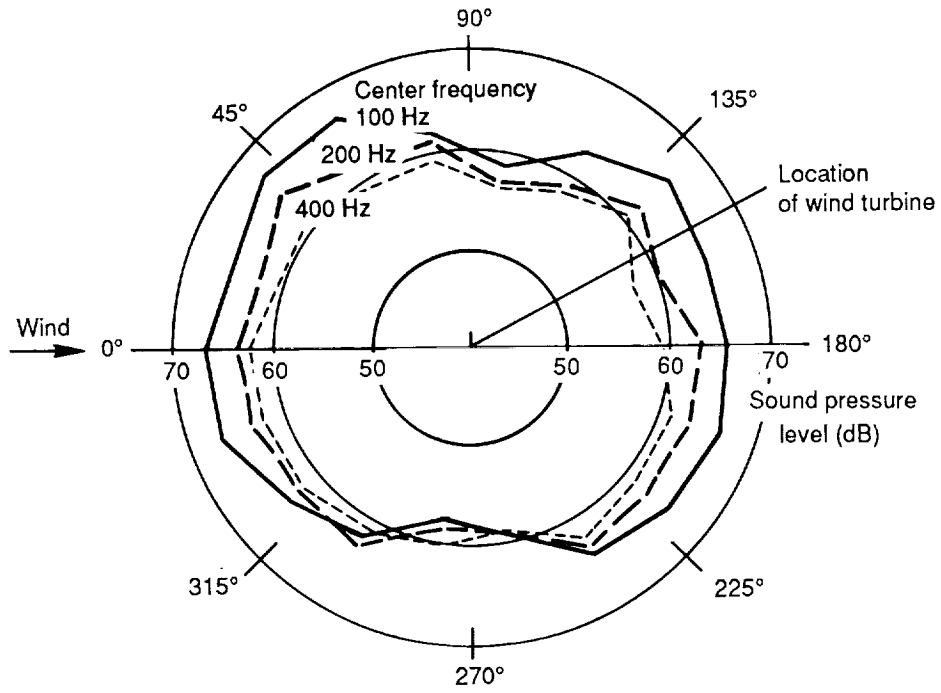

Figure 7-7. Example radiation patterns for broadband noise 200 m from a large-scale HAWT (one-third-octave bands, wind speed = 12.1 m/s, power = 2050 kW) [Shepherd, Willshire, and Hubbard 1988]

The one-third-octave band spectra of Figure 7-8 were obtained for wind speeds varying by a factor of two. At lower frequencies, dominated by the rotational harmonics, the highest levels are shown to be associated with the highest wind speeds and the highest power outputs. At higher frequencies, dominated by broadband components, there is no clear trend in relation to wind speed. This result is in contrast to a scaling law given in Sutherland, Mantey, and Brown [1987], in which the A-weighted sound pressure level increases in proportion to the logarithm of the wind speed, and this is verified by data from a group of several small wind turbines.

Figure 7-8 and the upper spectrum in Figure 7-4 both represent the acoustic output of the same wind turbine. The higher sound pressure levels in Figure 7-8 are the typical result of increasing the frequency bandwidth.

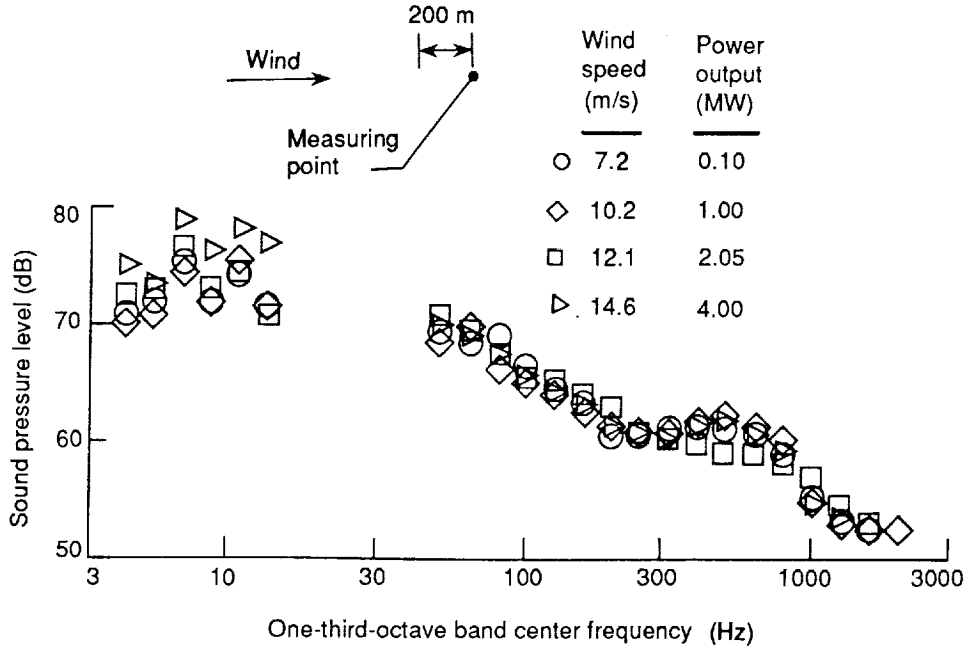

Figure 7-8. Typical variation in noise spectra with power output and wind speed 200 m from a large-scale HAWT (78.2-m diameter, downwind rotor) [Shepherd, Willshire, and Hubbard 1988]

Figures 7-9 and 7-10 contain measured data for several HAWTs of various sizes and configurations [Shepherd, Willshire, and Hubbard 1988]. In Figure 7-9 [Hubbard and Shepherd 1984], measured far-field data for several upwind-rotor turbines are adjusted to a distance of 2.5 rotor diameters from the base of the tower and are plotted as one-third-octave band spectra. The disk power densities (in W/m^2) and tip speeds for all of these machines are comparable, and the spectra (adjusted for distance) are in general agreement except at the lower frequencies. Comparable data are presented in Figure 7-10 for several downwind rotors [Shepherd *et al.* 1988; Hubbard and Shepherd 1982; Shepherd and Hubbard 1981; Lunggren 1984]; the results are similar. The variations in noise levels in Figure 7-10 can be related to the variations in rotor tip speed, as noted in the legend. A reference line of −10 dB per decade is included to indicate roughly the rate at which the broadband noise levels decrease as frequency increases.

Horizontal-axis turbines sometimes operate such that the wind direction is not aligned with the rotor axis. The effects of nonalignment, or skew, on the generated noise have been evaluated for a large-scale HAWT with a downwind rotor. Data are shown in Figure 7-11 for skew angles of 20° and 31° and are compared with sound pressure levels for 0° (no skew). The band levels plotted are arithmetic averages of measured values in the upwind and downwind quadrants. The obvious result is that sound pressure levels at low frequencies are reduced as the skew angle increases. This would be expected because of the reduced aerodynamic loading associated with an increased skew angle. At the higher frequencies, there are some small increases in the sound pressure levels as the skew angle increases. Such increases would be difficult to predict because the flow fields on the blades are very complicated.

In some situations, small tabs or vortex generators were installed on the low-pressure surfaces of both HAWT and VAWT blades to delay local stall and generally improve aerodynamic performance. Studies to evaluate the effects of vortex generators on noise radiation show the effects to be insignificant [Hubbard and Shepherd 1984].

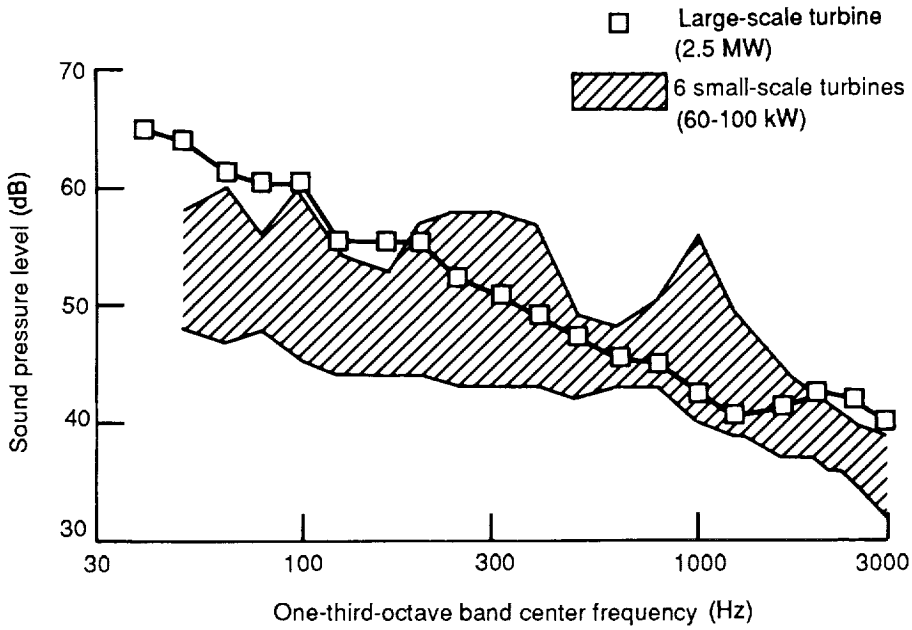

Figure 7-9. Noise spectra from small- and large-scale HAWTs with upwind rotors (downwind distance = 2.5 rotor diameters)

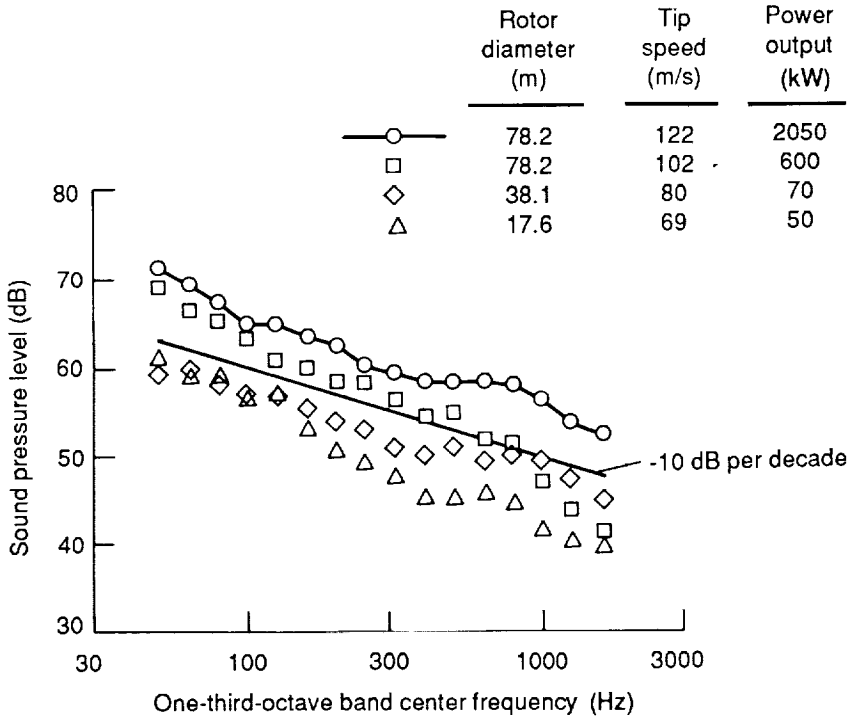

Figure 7-10. Noise spectra from small-, intermediate-, and large-scale HAWTs with downwind rotors (downwind distance = 2.5 rotor diameters) [Shepherd *et al.* 1988; Lunggren 1984; Shepherd and Hubbard 1981; Hubbard and Shepherd 1982]

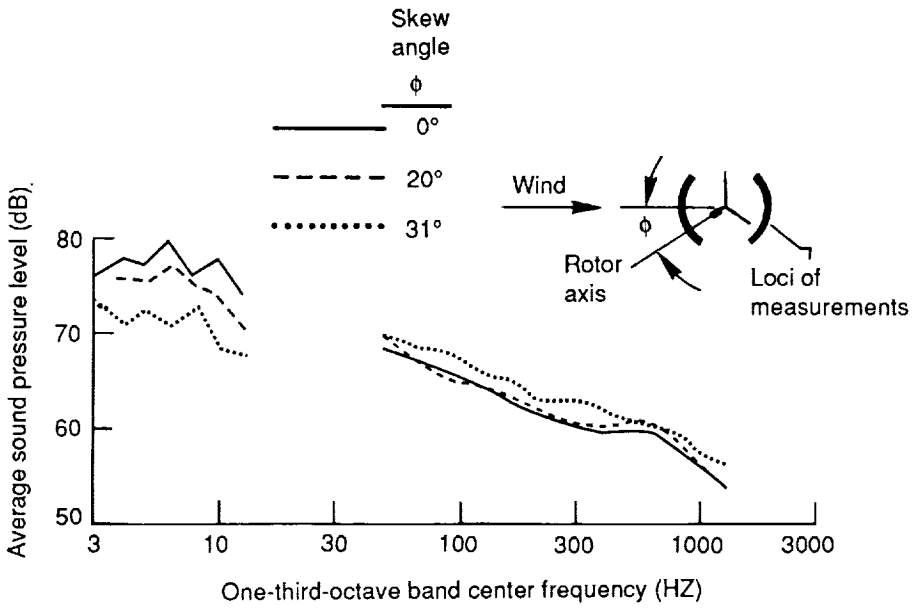

Figure 7-11. Effect of skew angle on the noise spectra of a large-scale HAWT with a downwind rotor [Shepherd, Willshire, and Hubbard 1988]

Noise from Aileron Control Surfaces

Some experimental HAWT blades have contained ailerons for speed and power control. Data for two different aileron configurations are given in Shepherd and Hubbard [1984]. The unusually high noise levels observed in these tests are believed to result from the excitation of internal cavity resonances in the blades by the external flow. Well-designed aileron systems would not have this problem.

Machinery Noises

Most of the acoustic noise associated with the large HAWTs studied to date has been aerodynamic in origin. Potential sources of mechanical noise, such as gears, bearings, and accessories, have not been important. However, for some of the smaller HAWTs and some VAWTs, gear noise can be an important component. Some straightforward approaches to controlling gear noise could be to include noise and vibration specifications in the design and to apply noise insulation around the gear box.

Narrow-band analyses of noise from a large HAWT (Figure 7-5) show identifiable components at the shaft speed of the generator (30 Hz) and at harmonics of this speed. Because these components radiate generally perpendicular to the axis of rotation and are not normally heard, they are of only secondary importance. Similarly, the cooling fan noise noted in Figure 7-4 is not significant.

Predicting Noise from A Single Wind Turbine

Extensive research studies have been conducted to predict noise from isolated airfoils, propellers, helicopter rotors, and compressors. Many of those findings have helped identify the significant noise sources of wind turbines and have helped develop methods for noise prediction. This section summarizes the technology available for predicting the known

sources of wind turbine noise, particularly the aerodynamic sources, which are believed to be the most important.

Rotational Harmonics

The generation of impulsive noise by a wind turbine is analogous to that of a propeller, compressor, or helicopter rotor. Impulse noises like those shown in Figures 7-3 and 7-4 can be resolved into their Fourier components (Figure 7-5), which are at the blade passage frequency and its integer multiples. For the example data, the harmonics occur at 1-Hz intervals—the blade passage frequency of this turbine. The acoustic pulses arise from rapidly changing aerodynamic loads on the blades as they traverse the wake of the support tower. The blades encounter localized flow deficiencies, which result in momentary fluctuations in lift and drag. Lift and drag coefficients can be transformed into thrust and torque coefficients, respectively, and can be used to determine the unsteady forces associated with periodic variations in the wind velocity. These variations may occur within the tower wake, as indicated schematically in Figure 7-3, or through wind shear.

Variations in blade force can be represented by complex Fourier coefficients modified by the Sears function to determine the effects of unsteady aerodynamics on the airfoil. The Sears function represents aerodynamic loading on a rigid airfoil passing through a sinusoidal gust [Sears 1941]. Following the method presented in Viterna [1981], a general expression for the RMS sound pressure level of the nth harmonic can be derived in a form that reduces to the following:

$$P_n = \frac{K_n\sqrt{2}}{4\pi d} \sum_m \left\{ e^{im[\phi-(\pi/2)]} J_x\ (K_n R_e \sin\gamma) \times \left(a_m^T \cos\gamma - \frac{nB-m}{K_n R_e}\ a_m^Q \right) \right\} \qquad (7\text{-}1)$$

where

P_n = RMS sound pressure for the nth harmonic (N/m^2)
n = sound pressure harmonic number ($n = 1, 2, \ldots$)

$K_n = \frac{nB\Omega}{a_o}$ (m^{-1})

B = number of blades
Ω = rotor speed (rad/s)
a_o = speed of sound (m/s)
d = distance from the rotor (m)
m = blade loading harmonic index ($m = \ldots, -2, -1, 0, 1, 2, \ldots$)
J_x = Bessel function of the first kind and of order x, in which $x = nB - m$
R_e = effective blade radius (m)
γ, ϕ = azimuth and altitude angles to the listener, referred to as the rotor thrust vector (rad)
a_m^T, a_m^Q = complex Fourier coefficients for the thrust and torque forces (acting at R_e), respectively (N)

Note that each loading harmonic m on the blade, because of fluctuating air loads, gives rise to more than one sound harmonic n in the radiation field.

For the special case in which the inflow to the rotor disk is uniform and the listener is located in the plane of the axis, Eq. 7-1 reduces to

$$P_n = \frac{K_n\sqrt{2}}{4\pi d}\left(T\cos\gamma - \frac{nBQ}{K_nR_e^2}\right)J_{nB}(K_nR_e\sin\gamma) \qquad (7\text{-}2)$$

where T and Q are the total thrust (in N) and torque (in N-m) of the rotor, respectively.

Example Rotational Noise Calculations

Examples of sound pressure levels calculated by means of Eq. 7-1 are presented in Viterna [1981] and are included in Figures 7-12 and 7-13. The calculations relate to the following operating conditions of the MOD-1 HAWT:

rotor speed	= 34.6 rpm	hub height	= 46 m
power output	= 1500 kW	listener distance	= 79 m and 945 m downwind from the rotor
wind speed	= 13.4 m/s		
rotor diameter	= 61 m	number of blades	= 2

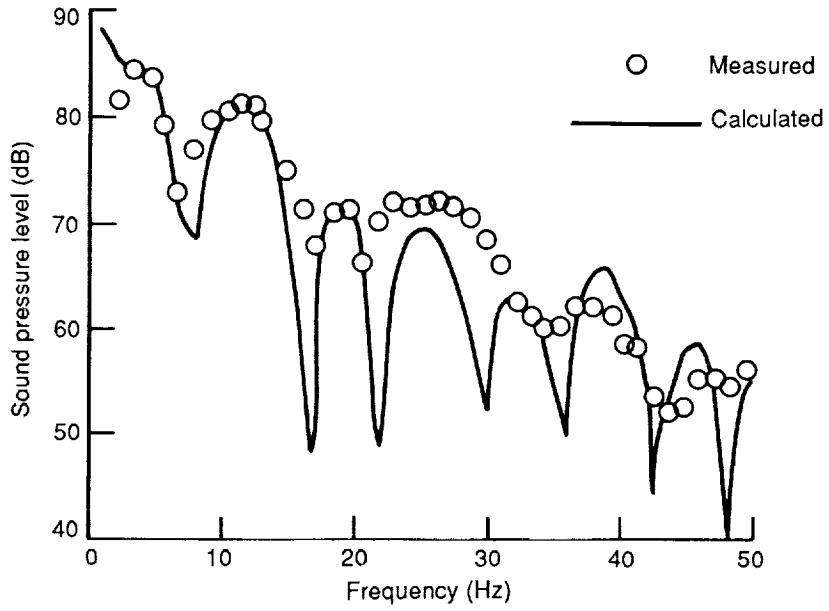

Figure 7-12. Measured and calculated rotational noise spectra 79 m downwind of the MOD-1 HAWT (rotor diameter = 61 m, wind speed = 13.4 m/s, power output = 1500 kW) [Viterna 1981]

The velocity deficiency behind the support tower was assumed to be 20% over a rotor disk azimuth angle of 20°.

Figure 7-12 compares calculated and measured sound pressure levels of the first 50 rotational harmonics for the MOD-1 downwind rotor. The calculations predict the maximum levels quite well, as well as the general shape of the spectrum. Other calculations [Viterna 1981] suggest that the maximum levels of the rotational harmonics occur in the upwind and downwind directions, while the minimum levels occur in the crosswind directions. Note that the calculation procedure presented in Eq. 7-1 has been validated for the MOD-1 and WTS-4 machines. Alternative methods for predicting the magnitude of

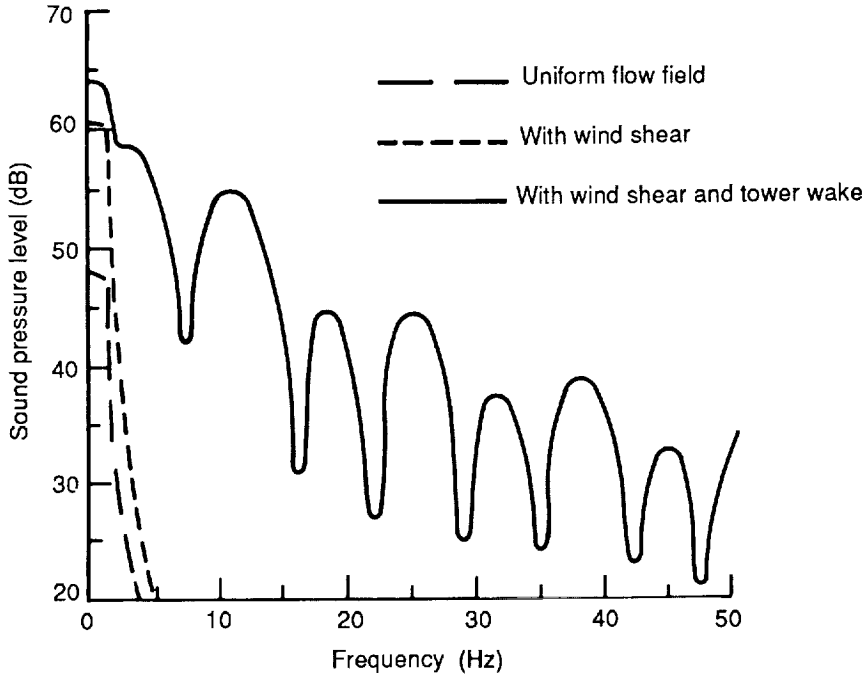

Figure 7-13. Calculated envelopes of rotational noise spectra for various wind inflow conditions 945 m downwind of the MOD-1 HAWT (rotor diameter = 61 m, wind speed = 13.4 m/s, power output = 1500 kW) [Viterna 1981]

rotational harmonics are discussed, and pertinent results are presented in Kelley *et al.* [1985]; Meijer and Lindblad [1983]; Greene and Hubbard [1980]; Martinez, Widnall, and Harris [1982]; George [1978]; and Lowson [1970].

Calculations made with Eq. 7-2 were compared with those for a nonuniform wind inflow, and the results are shown in Figure 7-13. For a uniform flow field, the fundamental rotational harmonic is relatively strong but all higher harmonics are weak. A similar result is obtained when the rotor operates in a shear flow that produces a once-per-revolution variation of inflow velocity at each blade. When tower wake effects are added, however, the levels of the higher frequencies are greatly enhanced.

These results suggest that both configuration and siting effects are significant in the rotational noise generation of wind turbines. For example, the tower wake of both VAWTs and downwind-rotor HAWTs can greatly enhance the strength of the rotational noise harmonics. Other deviations in wind inflow from a uniform velocity over the disk may also enhance the strength of the rotational harmonics for all rotor configurations. Flow deviations may be caused by the vertical wind velocity gradient in the earth's boundary layer and may be exaggerated by atmospheric turbulence or terrain features that can impose additional velocity gradients on the inflow.

Broadband Noise Components

Extensive research on propellers, helicopter rotors, compressors, and isolated airfoils has provided a wealth of background information and experience for predicting broadband noise for wind turbine rotors. The main noise sources have been identified, prediction techniques have been described, and comparisons have been made with available experimental data [George and Chou 1984; Glegg, Baxter, and Glendinning 1987;

Grosveld 1985]. Measurements to date indicate three main sources of broadband noise in wind turbine rotors:

1. Aerodynamic loading fluctuations caused by inflow turbulence interacting with the rotating blades
2. The turbulent boundary-layer flow over the airfoil surface interacting with the blade trailing edge
3. Vortex shedding caused by the bluntness of the trailing edge.

These sources of broadband noise are illustrated in Figure 7-14, along with their sound power dependencies, definitions of critical dimensions, and flow velocities [Grosveld 1985].

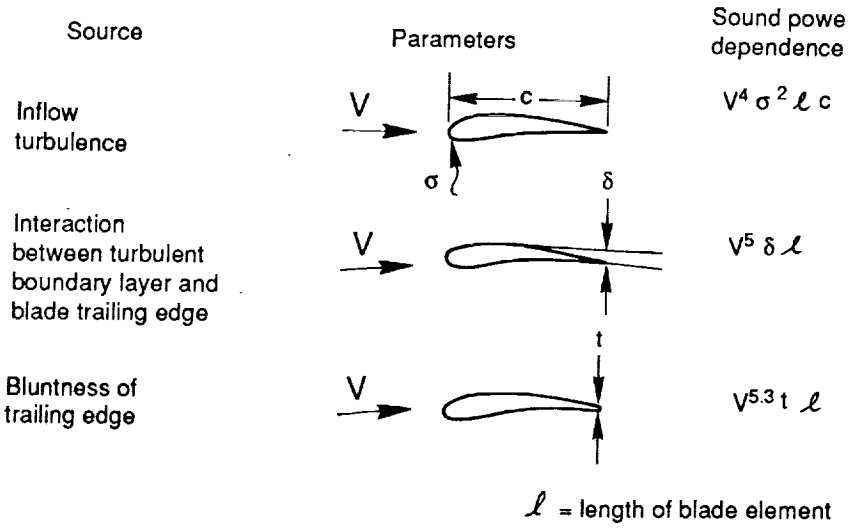

Figure 7-14. Sources of wind turbine broadband noise [Grosveld 1985]

Another possible source of broadband noise is that of tip vortex formation. Based on the experimental data of isolated airfoils and rotors [George and Chou 1984; Brooks and Marcolini 1986], this source is expected to be of secondary importance relative to the three listed. However, unusual geometries, such as those associated with tip control surfaces, could result in significantly more radiated noise.

Inflow Turbulence Noise

As the wind turbine blades move through the air, they encounter atmospheric turbulence that causes variations in the local angle of attack, which in turn causes fluctuations in the lift and drag forces. The length scales and intensities are a function of local atmospheric and site conditions and are different at different heights above the ground [Kelley *et al.* 1987]. The following expression for HAWT rotor noise induced by inflow turbulence is based on the work presented in Grosveld [1985]:

$$SPL_{1/3}(f) = 10 \log_{10} [B \sin^2 \Theta \rho^2 c_{0.7} R\sigma_2 V_{0.7}^4/(d^2 a_o^2)] + K_a \quad (7\text{-}3)$$

and

$$f_{peak} = SV_{0.7}/(h - 0.7R) \quad (7\text{-}4)$$

where

$SPL_{1/3}$ = one-third-octave band sound pressure level (dB)
f = band center frequency (Hz)
Θ = angle between the rotor-hub-to-receiver line and its vertical projection in the rotor plane (rad)
ρ = air density (kg/m^3)
$c_{0.7}$ = rotor blade chord at 0.7 radius (m)
R = rotor radius (m)
σ^2 = mean square of turbulence (m^2/s^2)
$V_{0.7}$ = blade forward speed at 0.7 radius, 0.7 RΩ (m/s)
Ω = rotor speed
K_a = frequency-dependent scaling factor (dB, Figure 7-15)
f_{peak} = frequency at which K_a is maximum (Hz, Figure 7-15)
S = constant Strouhal number, 16.6
h = hub height

A peak in the frequency domain is obtained when f reaches f_{peak}, which corresponds to the maximum value of $K_a(f)$ in Figure 7-15. Inherent in the derivation of Eq. 7-3 are the assumptions that the turbulence is isotropic and the atmosphere is neutrally stable within the vertical layer occupied by the rotor. In addition, the source is considered to be a point dipole at hub height, and the wavelength of the radiated sound is much shorter than the distance to the receiver. The frequency-dependent scaling factor in Figure 7-15 has been determined empirically from measured frequency spectra for a rotor from which the noise is largely caused by inflow turbulence.

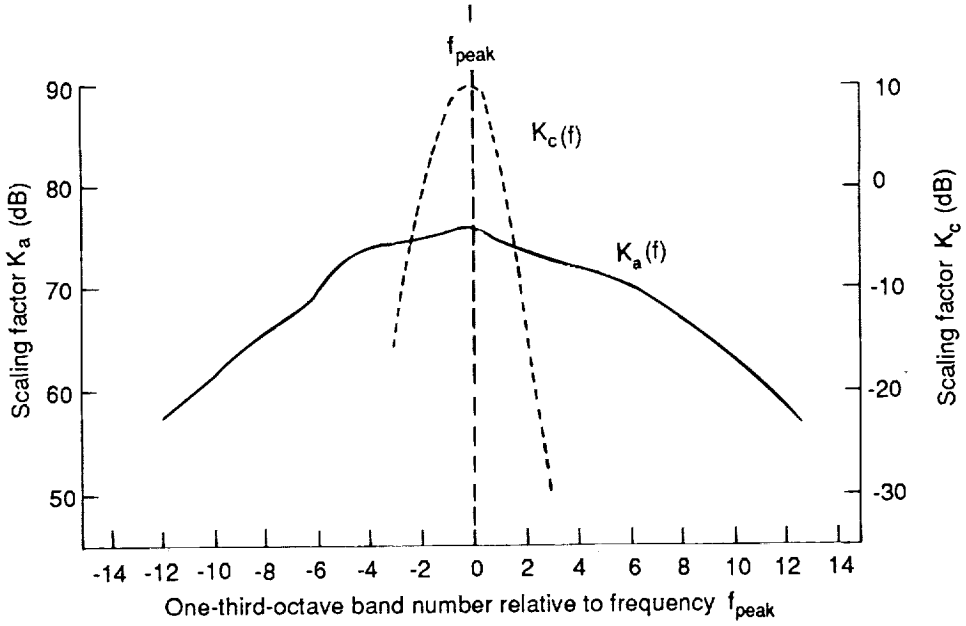

Figure 7-15. Predicted frequency-dependent scaling factors for broadband noise

Noise from the Interaction of the Turbulent Boundary Layer and the Blade Trailing Edge

Noise is generated by the convection of the blade's attached turbulent boundary layer into the wake of the airfoil. This is a major noise source for helicopter rotors, and the studies of Schlinker and Amiet [1981] have been adapted to wind turbine rotors. The resulting expression [Grosveld 1985] for an airfoil section is as follows:

$$SPL_{1/3}(f) = 10 \log_{10} \left\{ V_r^5 BD \frac{\delta l}{r_o^2} \left(\frac{S}{S_{max}}\right)^4 \left[\left(\frac{S}{S_{max}}\right)^{1.5} + 0.5 \right]^{-4} \right\} + K_b \quad (7\text{-}5)$$

where

V_r = resultant velocity at blade element (m/s)

D = directivity factor, $\dfrac{\sin^2(\theta/2)}{(1 + M\cos\theta)\,[1 + (M - M_c)\cos\theta]}$

θ = angle between the source-to-receiver line and its vertical projection in the rotor plane (rad)

M = airfoil Mach number, V_r/a_o

M_c = convection Mach number, 0.8 M

δ = boundary layer thickness, $\dfrac{0.37\,c}{R_n^{0.2}}$ (m)

c = blade chord (m)

R_n = Reynolds number, $\dfrac{V_r c}{\upsilon}$

ν = kinematic viscosity (m^2/s)

l = length of the blade element (m)

r_o = distance between the source and the receiver (m)

S = Strouhal number, $\dfrac{f\delta}{V_r}$

S_{max} = 0.1

K_b = constant scaling factor, 5.5 dB

Sound pressure levels are obtained by integrating contributions of all acoustic sources over the length of the blade.

Noise from Vortex Shedding at the Trailing Edge

Another noise source at the trailing edge of the airfoil is associated with vortex shedding caused by the bluntness of the trailing edge. This phenomenon is analogous to the shedding noise from wings with blunt trailing edges, as well as isolated airfoils, flat plates, and struts [Schlinker and Amiet 1981; Brooks and Hodgson 1980]. The expression derived in Grosveld [1985] for the noise from a blunt trailing edge is as follows:

$$SPL_{1/3}(f) = 10 \log_{10} \left\{ \frac{B\, V_r^{5.3}\, t1 \sin^2(\theta/2) \sin^2 \psi}{(1 + M \cos\theta)^3 [1 + (M - M_c) \cos\theta]^2 r_o^2} \right\} + K_c \quad (7\text{-}6)$$

and

$$f_{peak} = \frac{0.1\, V_r}{t} \quad (7\text{-}7)$$

where

t = trailing edge thickness (m)
ψ = angle between the source-to-receiver line and its horizontal projection in the rotor plane (rad)
K_c = frequency-dependent scaling factor (dB, Figure 7-15)

The corresponding K_c has its maximum value when f reaches f_{peak} (Figure 7-15). Once again, sound pressure levels are obtained by integrating the contributions of all acoustic sources over the length of the blade.

Example Calculations of Broadband Noise

Figure 7-16 illustrates the relative contributions of the broadband noise components calculated by using the methods of Grosveld [1985] for a large-scale HAWT with an upwind rotor. The calculations are in the form of one-third-octave band spectra for each of the broadband components identified. Also included is the summation of the components. As shown in Figure 7-16, inflow turbulence contributes noise over the whole frequency range and dominates the spectrum at frequencies below about 500 Hz. Effects of

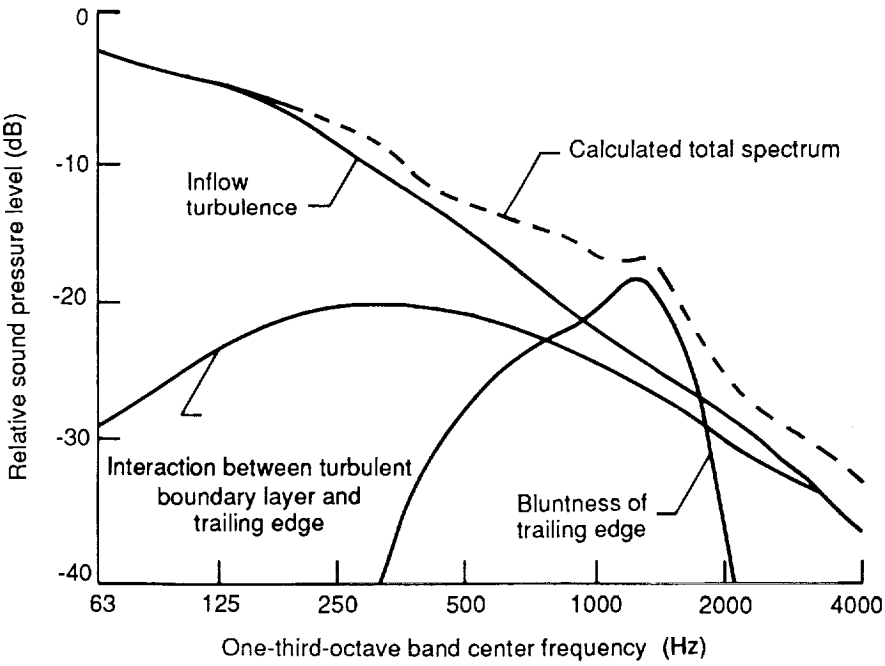

Figure 7-16. Relative contributions of broadband noise sources to the total noise spectrum calculated for a large-scale HAWT [Grosveld 1985]

boundary-layer interaction also contribute noise over a wide frequency range but are most significant at higher frequencies. On the other hand, the noise spectrum of the trailing edge wake is sharply peaked; the maximum for the example turbine is near 1250 Hz.

Figure 7-17 presents sound pressure levels calculated by using the methods of Grosveld and compares them with acoustic far-field measurements for a large, upwind-rotor HAWT and two different downwind-rotor HAWTs. Good agreement is shown in all cases. Note that the validation of Eqs. 7-3 to 7-7 has been limited to acoustic radiation in the upwind and downwind directions only.

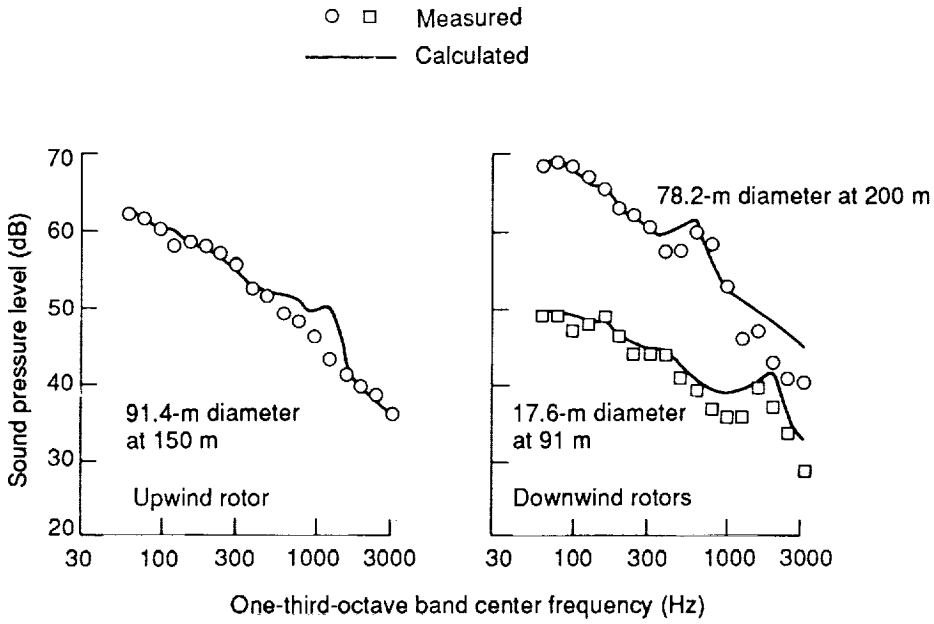

Figure 7-17. Measured and calculated broadband noise spectra downwind of various HAWTs [Grosveld 1985]

An alternative broadband-noise-prediction scheme is proposed in Glegg, Baxter, and Glendinning [1987] and includes unsteady lift noise, unsteady thickness noise, trailing edge noise, and noise from separated flows. Inflow turbulence at the rotor must be specified to predict unsteady lift and thickness noises. Using the turbulence data associated with the atmospheric boundary layer as input yielded poor agreement between calculated and measured noise levels. Thus, Glegg, Baxter, and Glendinning [1987] hypothesized that there was an additional source of turbulence: that each blade ran into the tip vortex shed by the preceding blade. Note that Grosveld [1985] also used atmospheric boundary layer turbulence but found that better agreement with acoutic measurements required an empirical turbulence model. The boundary layer and trailing edge noise formulations of Glegg, Baxter, and Glendinning [1987] and Grosveld [1985] both share the same theoretical background and therefore should give the same results.

Noise Propagation

A knowledge of the manner in which sound propagates through the atmosphere is basic to the process of predicting the noise fields of single and multiple machines. Although much is known about sound propagation in the atmosphere, one of the least

understood factors is the effect of the wind. Included here are brief discussions of the effects of distance from various types of sources, the effects of such atmospheric factors as absorption in air and refraction caused by sound speed gradients, and terrain effects.

Distance Effects

Point Sources

When there is a nondirectional point source as well as closely grouped, multiple point sources, spherical spreading may be assumed in the far radiation field. Circular wave fronts propagate in all directions from a point source, and the sound pressure levels decay at the rate of –6 dB per doubling of distance in the absence of atmospheric effects. The latter decay rate is illustrated by the straight line in Figure 7-18. The dashed curves in the figure represent increased decay rates associated with atmospheric absorption at frequencies significant for wind turbine noise.

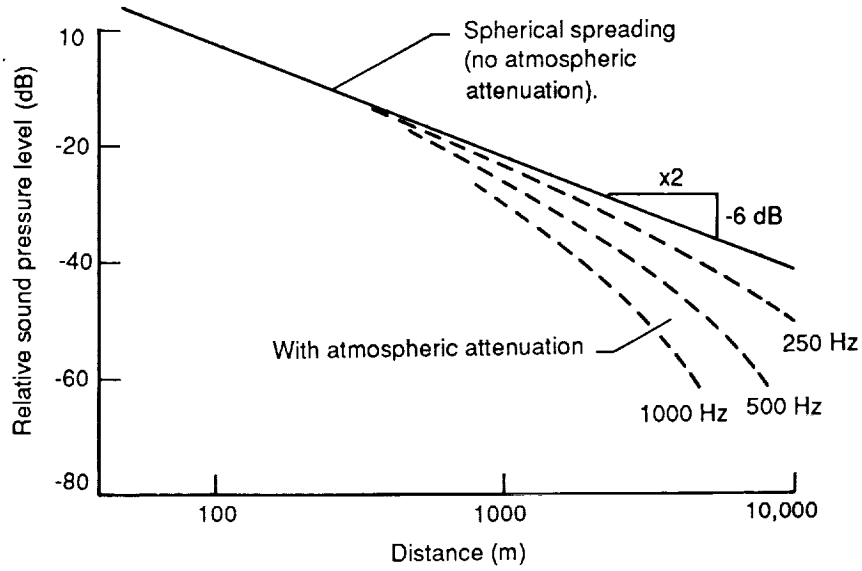

Figure 7-18. Decrease in sound pressure levels of pure tones as a function of distance from a point source [ANSI 1978]

Line Sources

For an infinitely long line source, the decay rate is only –3 dB per doubling of distance, compared with the –6 dB per doubling of distance illustrated in Figure 7-18. Such a reduced decay rate is sometimes observed for sources such as trains and lines of vehicles on a busy road. Some arrays of multiple wind turbines in wind power stations may also behave acoustically like line sources.

Atmospheric Factors

Absorption in Air

As sound propagates through the atmosphere, its energy is gradually converted to heat by a number of molecular processes such as shear viscosity, thermal conductivity, and molecular relaxation, and thus atmospheric absorption occurs. The curves in Figure 7-19 were plotted from ANSI values [1978] and show changes in atmospheric absorption as a function of frequency. In these examples, the ambient temperature varied from 0° to 20°C and the relative humidity varied from 30% to 70%. The atmospheric absorption is relatively low at low frequencies, increasing rapidly as a function of frequency. Atmospheric absorption values for other conditions of ambient temperature and relative humidity can be obtained from the ANSI tables; these values follow the general trend shown in Figure 7-19.

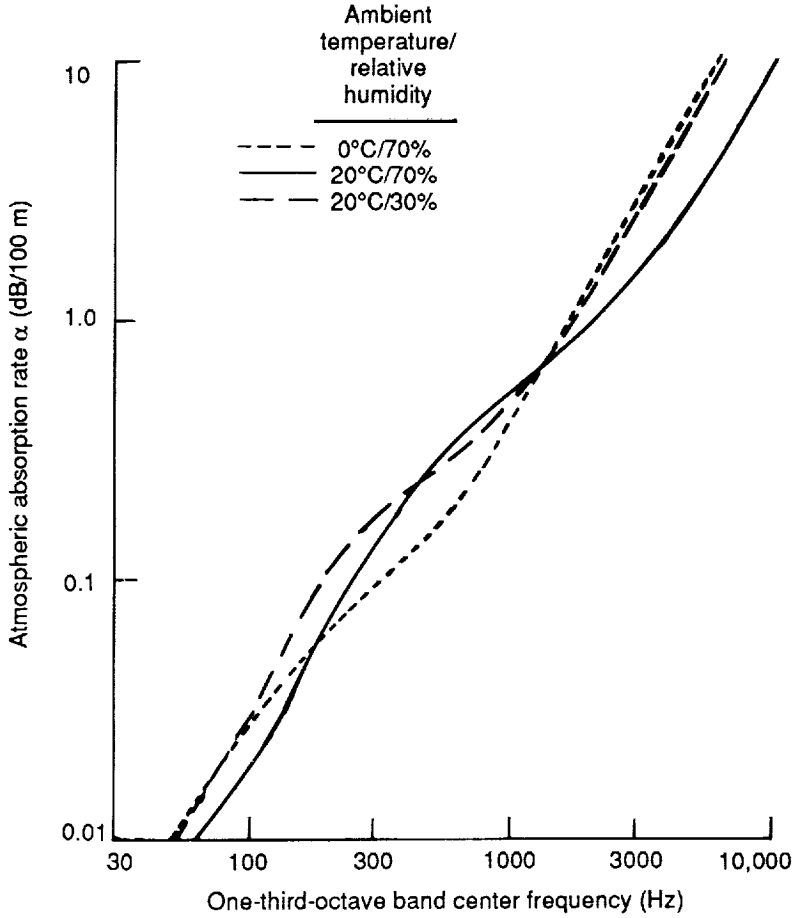

Figure 7-19. Standard rates of atmospheric absorption [ANSI 1978]

Refraction Caused by Wind and Temperature Gradients

Refraction effects arising from the sound speed gradients caused by wind and temperature can cause nonuniform propagation as a function of azimuth angle around a source. Figure 7-20 is a simple illustration of the effects of atmospheric refraction, or bending of

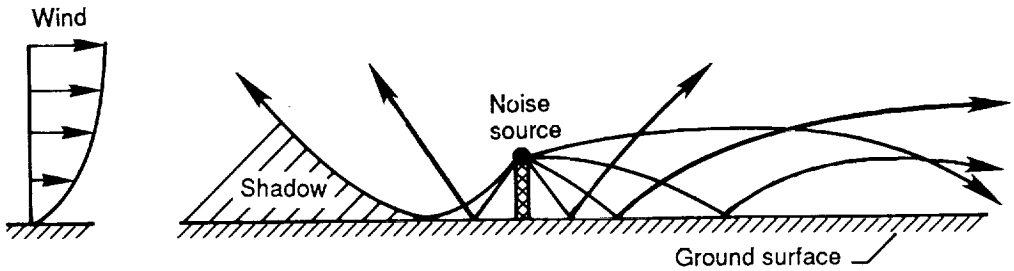

Figure 7-20. Effects of wind-induced refraction on acoustic rays radiating from an elevated point source [Shepherd and Hubbard 1985]

sound rays, caused by a vertical wind-shear gradient over flat, homogeneous terrain for an elevated point source. Note that in the downwind direction the wind gradient causes the sound rays to bend toward the ground, whereas in the upwind direction the rays curve upward away from the ground. For high-frequency acoustic emissions, this causes greatly increased attenuation in a shadow zone upwind of the source, but little effect downwind. The attenuation of low-frequency noise, on the other hand, is reduced by refraction in the downwind direction, with little effect upwind.

The distance from the source to the edge of the shadow zone is related to the wind-speed gradient and the elevation of the source. In a 10- to 15-m/s wind, for a source height from 40 to 120 m above flat, homogeneous terrain, the horizontal distance from the source to the shadow zone was calculated to be approximately five times the height of the source [Shepherd and Hubbard 1985].

Attenuation exceeding that predicted by spherical spreading and atmospheric absorption can be found in the shadow zone. This attenuation is frequency-dependent, and the lowest frequencies are the least attenuated. Figure 7-21 presents an empirical scheme for estimating attenuation in the shadow zone, based on information in Piercy, Embleton, and Sutherland [1977]; SAE [1966]; and Daigle, Embleton, and Piercy [1986]. The estimated

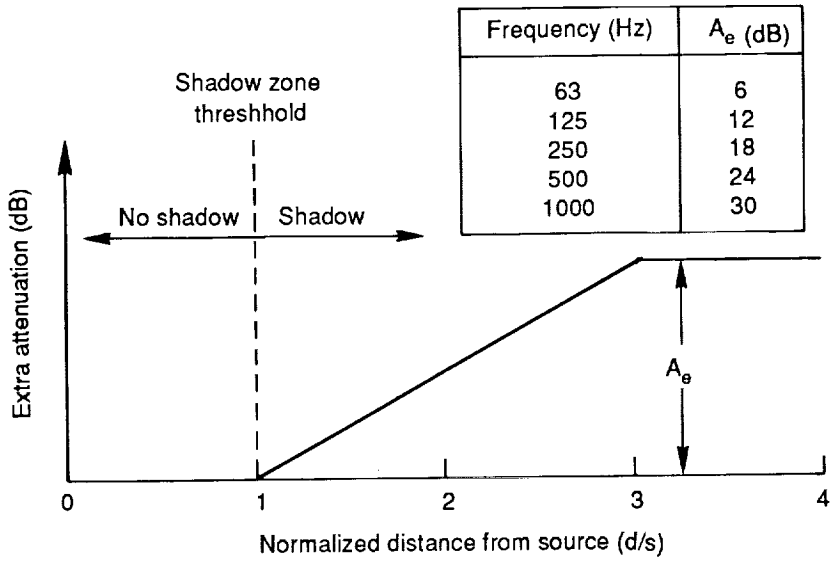

Figure 7-21. Empirical model for estimating the extra attenuation of noise in the shadow zone upwind of an elevated point source ($s = 5h$, $40 \leq h \leq 120$ m, where h = source elevation) [Shepherd and Hubbard 1985]

extra attenuation (A_e in Figure 7-21) is assumed to take place over a distance equal to twice that from the source to the edge of the shadow zone. The predicted decay in the sound pressure level from the source to the edge of the shadow zone is caused by atmospheric absorption [ANSI 1978] and spherical spreading. Within the shadow zone, extra attenuation should be added as estimated according to Figure 7-21.

Note that vertical temperature gradients, which are also effective sound speed gradients, will normally also be present. These will add to or subtract from the effects of wind that are illustrated in Figure 7-21. Effects of wind gradient will generally dominate those of temperature gradients in noise propagation from wind power stations.

Distributed Source Effects

Because of their large rotor diameters, some wind turbines exhibit distributed source effects relatively close to the machines. Only when listeners are at distances from the turbines that are large in relation to the rotor diameter does the rotor behave acoustically as a point source. As indicated in Figure 7-22, distributed source effects are particularly important in the upwind direction. In this figure, sound pressure levels in the 630-Hz, one-third-octave band are presented as a function of distance in the downwind, upwind, and crosswind directions. The measured data agree well with the solid curves, which represent spherical spreading and atmospheric absorption in the downwind and crosswind directions. In the upwind direction, however, the measured data fall below the solid curve; this

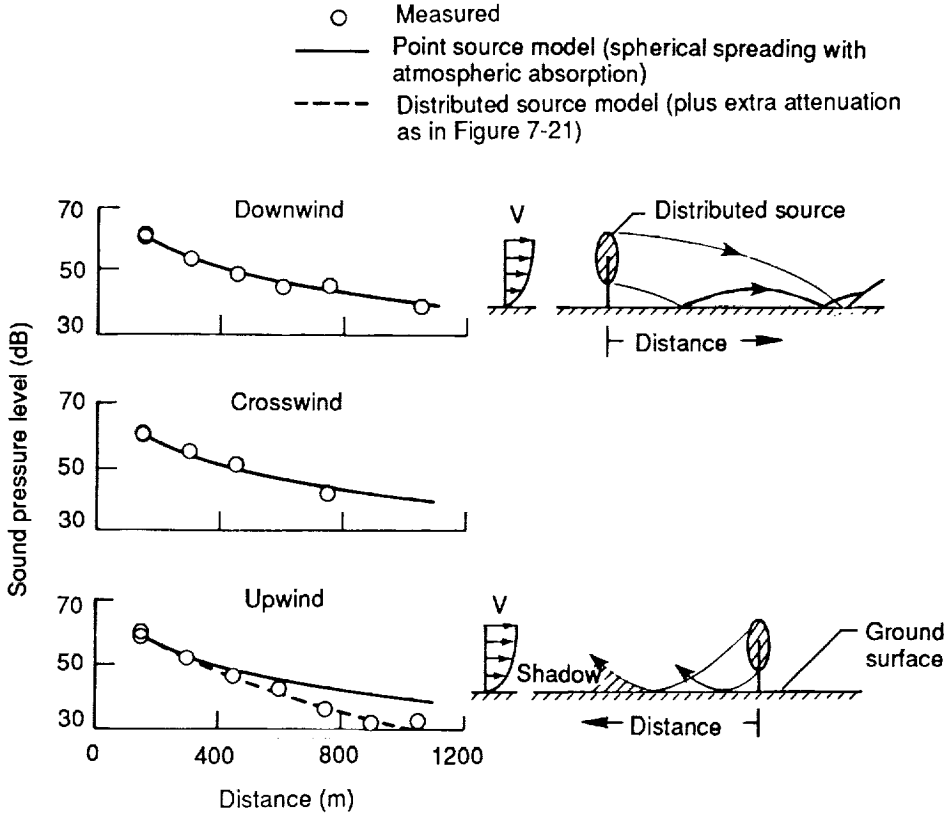

Figure 7-22. Measured and calculated sound pressure levels in three directions from a large-scale HAWT (one-third-octave band = 630 Hz, rotor diameter = 78.2 m) [Shepherd and Hubbard 1985]

indicates the presence of a shadow zone. An improvement in predicting upwind sound pressure levels is obtained when the noise source is modeled as being distributed over the entire rotor disk. Each part of the disk is then considered to be a point source, and attenuation is estimated by means of the empirical model shown in Figure 7-21. The resulting predictions are shown as the dashed curve of Figure 7-22 and are in good agreement with the sound measurements upwind of the turbine. In the downwind and crosswind directions, point-source and distributed-source models result in identical calculations of sound pressure levels.

Channeling Effects at Low Frequencies

Figure 7-23 illustrates the special case of propagation of low-frequency rotational-harmonics when the atmospheric absorption and extra attenuation in the shadow zone are very small. Measured sound pressure levels are shown as a function of distance for both the upwind and downwind directions. For comparison, the curves representing decay rates of –6 dB and –3 dB per doubling of distance are also included. Note that in the upwind case the sound pressure levels tend to follow a decay rate of –6 dB per doubling of distance, which is equal to the rate for spherical spreading. No extra attenuation from a shadow zone was measured.

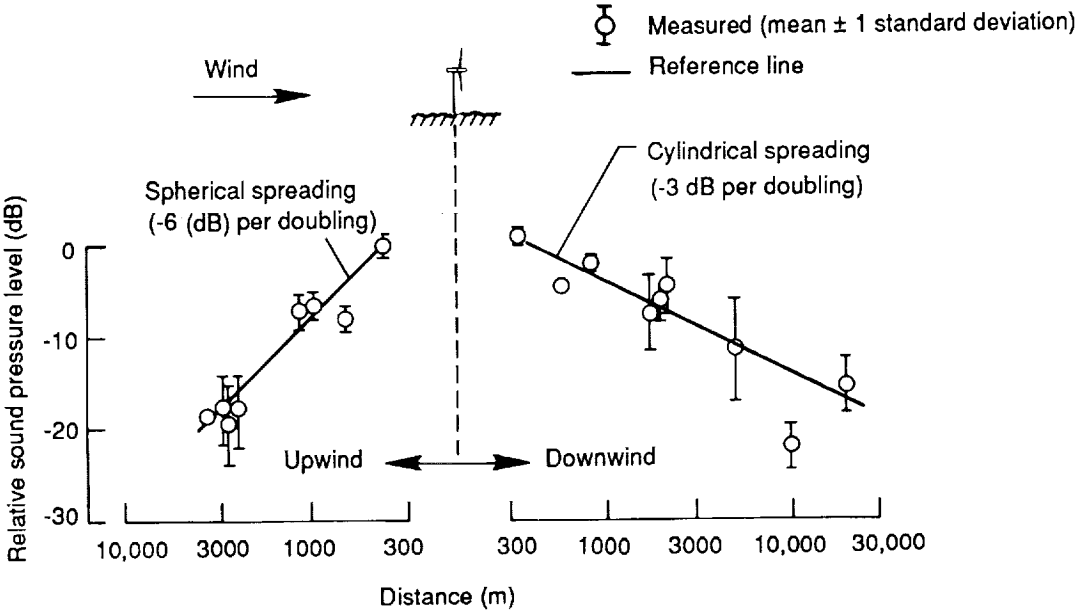

Figure 7-23. Measure effect of wind on the propagation of low-frequency rotational harmonic noise from a large-scale HAWT (harmonics with frequencies from 8 to 16 Hz, rotor diameter = 78.2 m) [Willshire and Zorumski 1987]

In the downwind direction, the sound pressure levels tend to follow a decay rate of –3 dB per doubling of distance, similar to that for cylindrical spreading. This reduced decay rate in the downwind direction at very low frequencies is believed to result from atmospheric refraction, which introduces a channeling sound path in the lower portions of the earth's boundary layer [Willshire and Zorumski 1987; Thomson 1982; Hawkins 1987].

Terrain Effects

Terrain effects include ground absorption, reflection, and diffraction. Furthermore, terrain features may cause complex wind gradients, which can dominate noise propagation to large distances [Kelley *et al.* 1985; Thompson 1982]. Wind turbines are generally located in areas devoid of trees and other large vegetation. Instead, ground cover usually consists of grass, sagebrush, plants, and low shrubs, which are minor impediments to noise propagation except at very high frequencies. At frequencies below about 1000 Hz, the ground attenuation is essentially zero.

Methods are available for calculating the attenuations provided by natural barriers such as rolling terrain, which may interrupt the line of sight between the source and the receiver [Piercy and Embleton 1979]. However, very little definitive information is available regarding the effectiveness of natural barriers in the presence of strong, vertical wind gradients. Piercy and Embleton [1979] postulate that the effectiveness of natural barriers in attenuating noise is not reduced under conditions of upward-curving ray paths (as would apply in the upwind direction) or under normal temperature-lapse conditions. However, under conditions of downward-curving ray paths, as in downwind propagation or during temperature inversions (which are common at night), the barrier attenuations may be reduced significantly, particularly at large distances.

Predicting Noise from Multiple Wind Turbines

Methods are needed to predict noise from wind power stations made up of large numbers of machines, as well as for a variety of configurations and operating conditions. This section reviews the physical factors involved in making such predictions and presents the results of calculations that illustrate the sensitivity of radiated noise to various geometric and propagation parameters. A number of valid, pertinent, simplifying assumptions are presented. A logarithmic wind gradient is assumed, with a wind speed of 9 m/s at hub height. Flat, homogeneous terrain, devoid of large vegetation, is also assumed. Noises from multiple wind turbines are assumed to add together incoherently, that is, in random phase.

Noise Sources and Propagation

Reference Spectrum for a Single Wind Turbine

The most basic information needed to predict noise from a wind power station is the noise output of a single turbine. Its noise spectrum can be predicted from knowledge of the geometry and operating conditions of the machine [Viterna 1981; Glegg, Baxter, and Glendinning 1987; Grosveld 1985], or its spectrum can be measured at a reference distance. Figures 7-9 and 7-10 are examples of spectral data for HAWTs. Also shown in Figure 7-10 is a hypothetical spectrum used in subsequent example calculations to represent a HAWT with a 15-m rotor diameter and a rated power of approximately 100 kW. The example spectrum is the solid line with a decrease of 10 dB per decade in sound pressure level with increasing frequency. This spectral shape is generally representative of the aerodynamic noise radiated by wind turbines. However, predictions for a specific wind power station should be based, if possible, on data for the particular types of turbines in the station.

Directivity of the Source

Measurements of aerodynamic noise for a number of large HAWTs (for example, Kelley *et al.* [1985]; Hubbard and Shepherd [1982]; and others listed in the bibliography) indicate that the source directivity depends on specific noise-generating mechanisms. For broadband noise sources, such as inflow turbulence and interactions between the blade boundary layer and the blade trailing edge, the sound pressure level contours at close distances are approximately circular. Lower-frequency, impulsive noise, which results when the blades interact with the tower or central column wake, radiates most strongly in the upwind and downwind directions.

Although there is one prevailing wind direction at most wind turbine sites, it is not uncommon for the wind vector to vary 90° in azimuth angle during normal operations. Therefore, one of the simplifying assumptions made in the calculations that follow is that each individual machine behaves like an omnidirectional source.

Considerations for Frequency Weighting

A-weighted sound pressure levels, expressed in dB(A), are in widespread use in evaluating the effects of noise on communities [Pearsons and Bennett 1974]. Figure 7-24 shows the results of applying this descriptor. The assumed single-turbine reference spectrum, at a distance of 30 m from the machine, is reproduced from Figure 7-10 as the solid line. The equivalent A-weighted spectrum at the same distance is shown as the upper dashed curve. This particular weighting emphasizes the higher frequencies and deemphasizes the lower frequencies according to the sensitivity of the human ear. As distances increase, as illustrated in the other dashed curves, atmospheric absorption causes the levels of the higher-frequency components to decay faster than those of the lower frequencies (see Figure 7-19). The result is that the midrange frequencies (100 to 1000 Hz) tend to dominate the A-weighted spectrum at large distances. Frequencies higher than 1000 Hz will generally not be important considerations at large distances because of the effects of atmospheric absorption. Frequency components below about 100 Hz may not be

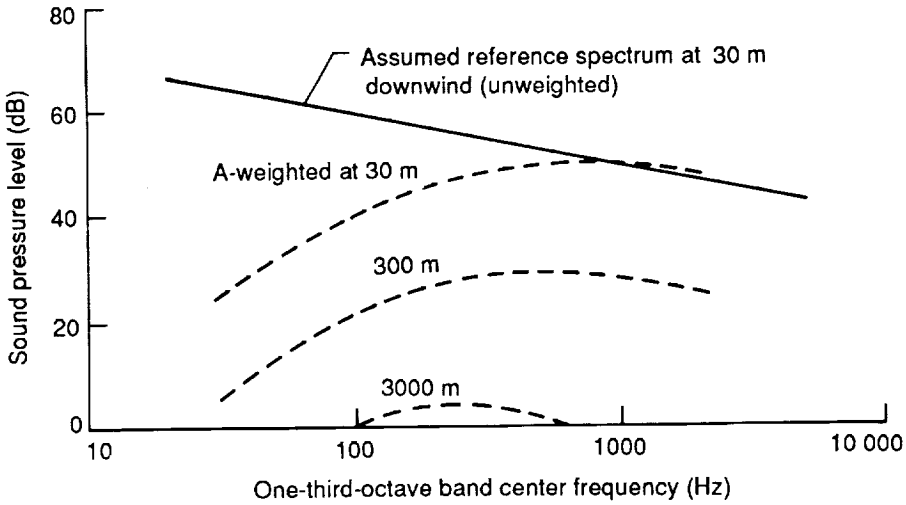

Figure 7-24. Reference and A-weighted noise spectra from a 15-m-diameter HAWT with a rated power of 100 kW (assumed for example calculations of noise from a wind power station)

significant in terms of audible noise, but they can be significant in terms of such indirect effects as noise-induced building vibrations.

Arrangement of Wind Power Stations

A basic geometric arrangement of wind turbines was assumed to represent an example wind power station (shown in Figure 7-25). The station consists of 31 turbines per row. Each machine produces approximately 100 kW of power, and the rotor diameter is 15 m. The spacing between turbines is 30 m, the row length is 900 m, and the spacing between rows is 200 m. The basic four-row configuration in Figure 7-25 was perturbed to investigate the effects of such variables as the number of rows, row and turbine spacing, row length, and turbine power rating.

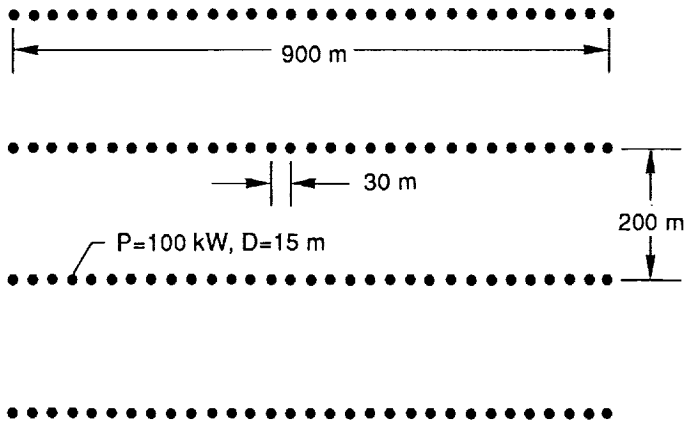

Figure 7-25. Layout of wind turbines in the example wind power station [Shepherd and Hubbard 1986]

Absorption and Refraction

These example calculations assumed an ambient temperature of 20°C and a relative humidity of 70%. From the data in Figure 7-19, assumed values of atmospheric absorption of 0, 0.10, 0.27, and 0.54 dB per 100 m correspond roughly to one-third-octave band center frequencies of 50, 250, 500 and 1000 Hz, respectively, for these temperature and humidity conditions. These frequencies were chosen because they encompass the range of frequencies considered important in evaluating the perception of wind turbine noise in adjacent communities [Shepherd and Hubbard 1986].

Calculation Methods

The method presented here for calculating the sound pressure level from incoherent addition is a sum of the random-phase multiple noise sources at any arbitrary receiver distance. This method assumes that each source radiates equally in all directions. Attenuation caused by atmospheric absorption is included; propagation is over flat, homogeneous terrain; and there is a logarithmic wind-speed gradient. The method has no limitations on the number of wind turbines or their geometric arrangements. The required input is a reference sound-pressure-level spectrum $L_o(f)$, either narrow-band or one-third-octave band,

for a single wind turbine. This spectrum can be measured or predicted for a reference distance from the rotor hub of approximately 2.5 times the rotor diameter.

The sound pressure level received from an individual wind turbine in the array in a given frequency band can be calculated with the following equation:

$$L_n(f_i) = L_o(f_i) - 20 \log_{10} (d_n/d_o) - \alpha(d_n - d_o)/100 \quad (7\text{-}8)$$

where

$L_n(f_i)$ = sound pressure level from the nth wind turbine (dB)
n = wind turbine index (1, 2, . . ., N)
N = number of wind turbines in the array
f_i = center frequency of the ith band (Hz)
$L_o(f_i)$ = reference sound pressure level in the ith frequency band from a single wind turbine at the reference distance (dB)
d_n = distance from the nth turbine to the receiver (m)
d_o = reference turbine-to-receiver distance (m)
α = atmospheric absorption rate (dB per 100 m)

The total sound pressure level, from all wind turbines in the array in the ith frequency band, is then calculated as follows:

$$SPL_{tot}(f_i) = 10 \log_{10} \sum_n 10^{L_n(f_i)/10} \quad (7\text{-}9)$$

This procedure can be repeated for all frequency bands to provide a predicted spectrum of sound pressure level at the receiver location. Noise measures such as the A-weighted sound pressure level may also be calculated by adding the A-weighting corrections at each frequency to the values of $L_n(f_i)$ or $SPL_{tot}(f_i)$ in Eqs. 7-8 and 7-9. If the sources are arranged in rows, the required computations can be reduced by using the simplified procedures of Shepherd and Hubbard [1986].

Examples of Calculated Noise for Wind Power Stations

A series of parametric calculations of unweighted sound pressure levels was performed based on the array of Figure 7-25 and systematic variations of that array [Shepherd and Hubbard 1986]. The receiver is assumed to be on a line of symmetry either in the downwind, upwind, or crosswind direction.

Effect of Distance from a Single Row

Figure 7-26 shows calculated sound pressure levels for one row of the example wind power station, as a function of downwind distance for various rates of atmospheric absorption. Also shown are reference decay rates of –3 dB and –6 dB per doubling of distance. For an atmospheric absorption rate of zero, the decay rate is always less than that for a single point source (Figure 7-18). At intermediate distances, the row of turbines acts as a line source, for which the theoretical decay rate is –3 dB per doubling of distance or –10 dB per decade of distance. Only at distances greater than one row length (900 m) does the decay rate approach the single-point-source value of –6 dB per doubling of distance (–20 dB per decade). Decay rates increase as the absorption coefficient increases.

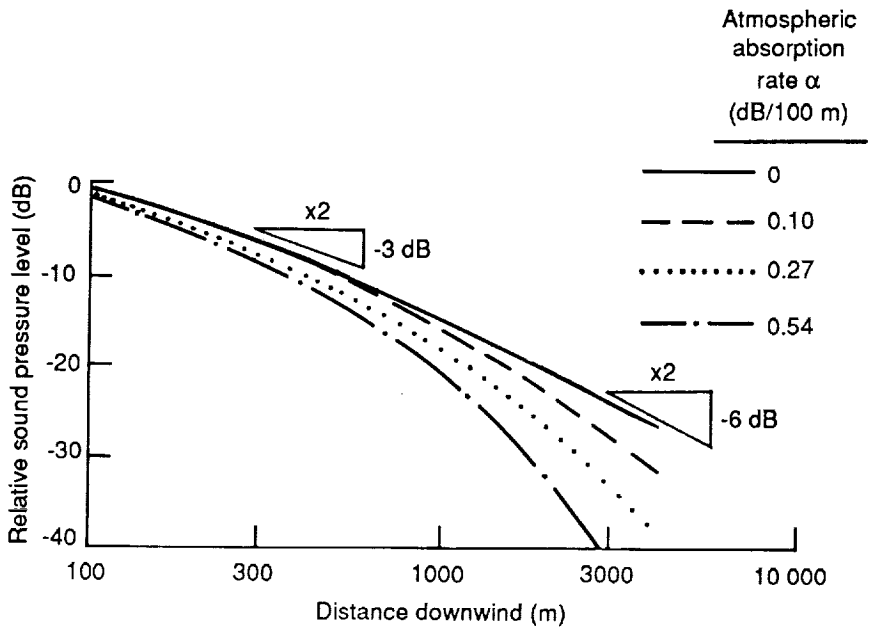

Figure 7-26. Calculated noise propagation downwind of a single row of wind turbines in the example array for four atmospheric absorption rates [Shepherd and Hubbard 1986]

Effect of Multiple Rows

Figure 7-27 presents the results of sound-pressure-level calculations that were made for one, two, four, and eight rows of wind turbines; this illustrates the effects of progressively doubling the number of machines for a constant turbine spacing. At zero atmospheric absorption, and at receiver distances that are large relative to the array dimensions, a doubling of the number of rows results in an increase of 3 dB in the sound pressure level.

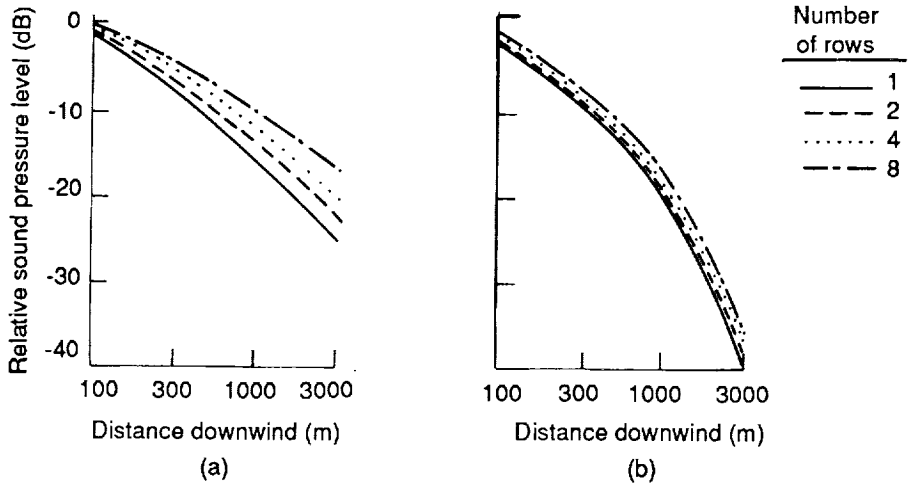

Figure 7-27. Calculated noise propagation downwind of various numbers of rows of wind turbines in the example array [Shepherd and Hubbard 1986]. (a) without atmospheric absorption. (b) $\alpha = 0.54$ dB/100 m.

This simply reflects a doubling of acoustic power. At shorter distances, the closest machines dominate and the additional rows result in only small increments in the sound pressure level.

For nonzero atmospheric absorption, the effect of additional rows is less significant at all receiver distances. Doubling the number of rows results in an increase in the sound pressure level of less than 3 dB.

Figure 7-28 shows similar data for two different row lengths. For these comparisons, the turbine spacing is constant and the row lengths are doubled by doubling the number of machines per row. When the receiver is at shorter distances, the predicted sound pressure levels are equal because of the equal turbine spacing. At longer distances, the levels for the double-length row are higher by 3 dB because the acoustic power per row is doubled.

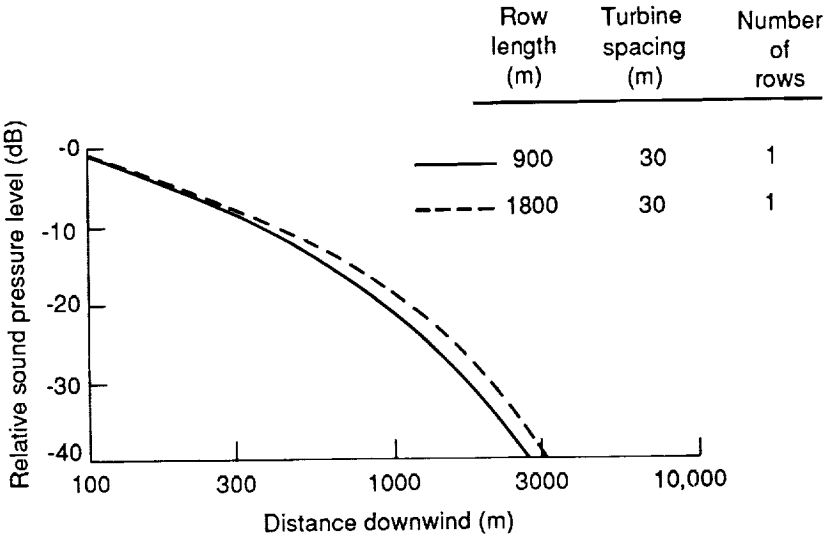

Figure 7-28. Calculated noise propagation downwind of wind turbines in rows of two different lengths (α = 0.54 dB/100 m) [Shepherd and Hubbard 1986]

Computations were also made [Shepherd and Hubbard 1986] for a configuration similar to that of Figure 7-25, except that the row spacing was reduced from 200 m to 100 m. At all distances to the receiver, the computed sound pressure levels were higher for this more compact array.

Effect of Turbine Rated Power

Shepherd and Hubbard [1986] calculate the effect of the turbine's rated power on noise emissions by increasing the power of each turbine and the total station power. The turbine and row spacings were adjusted from those of Figure 7-25 to more appropriate values for larger machines (four times the rated power). Sound pressure levels from rows of 16 400-kW wind turbines were compared with levels from the same number of rows of 31 100-kW machines. This approximately doubled the rated power of the station. The reference spectrum for the larger turbines was assumed to have the same shape as that of the smaller turbines (Figure 7-10), although the levels were all 6 dB higher. This implies four times the acoustic power for four times the rated power. The computed sound pressure levels are 3 dB higher for the array of larger turbines because the acoustic power is doubled for each row of the array. Different results would be obtained if the reference spectra of the two sizes of turbines had different shapes.

Directivity Considerations for a Wind Power Station

Although the individual turbines have been treated as if they radiate sound equally in all directions, an array of such sources may not have uniform directivity characteristics. Figure 7-29 compares the predicted sound pressure levels for two array configurations as received from two different directions. Calculations are presented for a receiver located downwind on the line of symmetry perpendicular to the rows and for a receiver located crosswind on the line of symmetry parallel to the rows. For the case of one row of turbines, the crosswind sound pressure level is predicted to be about 5 dB lower than the downwind level near the turbines, and only about 2 dB lower in the far field. For an array with eight rows, the crosswind sound pressure level is only 3 dB lower near the turbines, and there is little directivity once the receiver distance exceeds 300 m. Downwind levels are higher close to the eight-row array because the turbine spacing in the row is less than the row spacing.

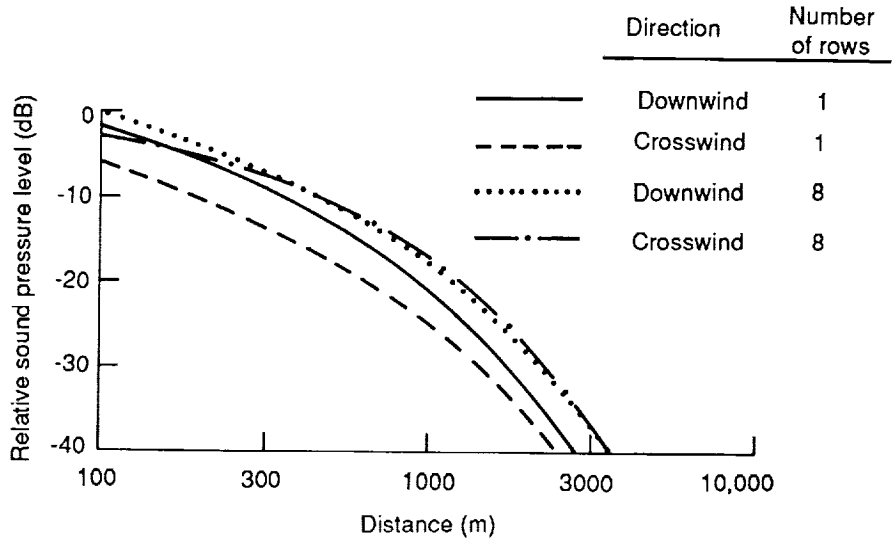

Figure 7-29. Calculated noise propagation downwind and crosswind of single and multiple rows of wind turbines in the example array (α = 0.54 dB/100 m) [Shepherd and Hubbard 1986]

Complete contours of sound pressure level around a wind power station were estimated (Figure 7-30). The array geometry was five rows of 31 machines each, spaced as shown in Figure 7-25. This gives an approximately square array. Figure 7-30 shows predicted contours for sound pressure levels of 40, 50, and 60 dB for an atmospheric absorption of 0.54 dB/100 m (which corresponds to a frequency of 1000 Hz at 20°C and 70% relative humidity). Assuming a hub-height wind speed of 9 m/s, the distances to contours in the upwind direction are greatly reduced. These upwind contours are derived from computed distances to the acoustic shadow zone and the extra attenuation that occurs within this zone (see Figure 7-21). An acoustic shadow zone forming upwind of the array results in greatly reduced distances to particular noise level contours for all frequencies above about 60 Hz. The dashed curve in Figure 7-30 shows the location of the 40-dB contour in the absence of a shadow zone.

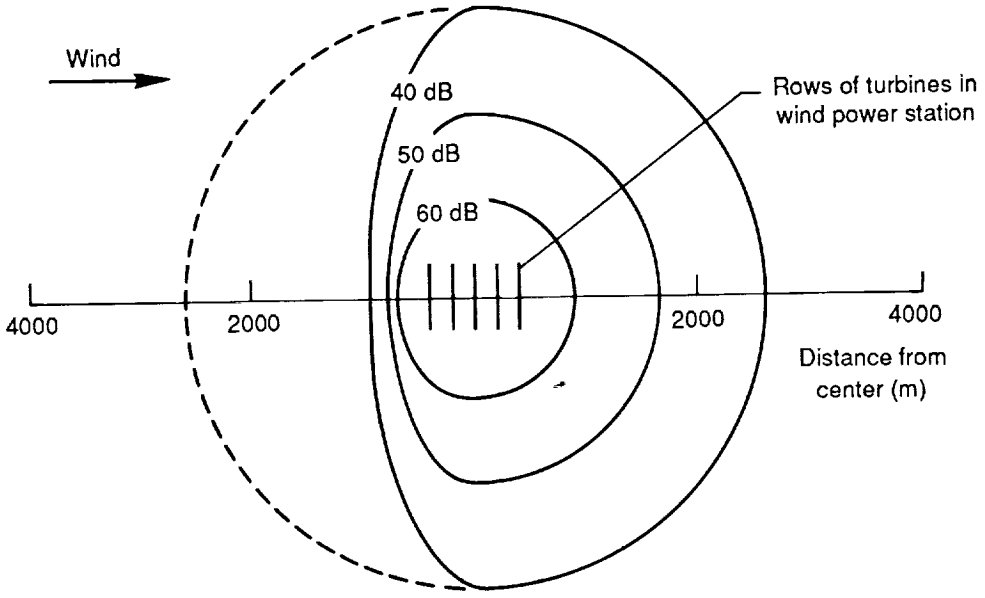

Figure 7-30. Calculated contours of sound pressure level around a five-row example array for the one-third-octave band at 1000 Hz (α = 0.54 dB/100 m) [Shepherd and Hubbard 1986]

A-Weighted Composite Spectra

The data of Figures 7-26 through 7-30 are derived for a few selected values of atmospheric absorption; the figures show how the noises from individual turbines sum incoherently for various arrays of machines. The particular absorption values used correspond to conditions of 20°C ambient temperature and 70% relative humidity (see Figure 7-19). Figure 7-31 illustrates the effects of A-weighting the composite sound spectrum from the example wind power station. Predicted sound spectra for the array are compared with equivalent spectra for a single machine (Figure 7-24). At large distances, the midrange frequencies dominate the A-weighted spectrum for both the single turbine and the array.

Receiver Response

Evaluating the effects of receivers' exposure to noise at various locations involves determining people's responses to direct acoustic radiation as well as the acoustic and vibrational environments inside buildings. The factors involved in such an evaluation are shown in Figure 7-32 and are explained in detail in Stephens *et al.* [1982]. Noise radiated by the wind turbine is propagated through the atmosphere to a receiver (a person or a building). The characteristics of the receiver then determine the acoustic and the vibration effects of the noise. The broadband and impulsive components of the acoustic response are treated separately, and both may be significant. Background noise and building vibrations must also be considered in evaluating people's responses to wind turbine noise.

If the wind turbine noise levels are below the corresponding background noise levels, they will generally not be perceived; therefore, no adverse human response is expected. When any noise level exceeds the threshold of perception, however, there is the potential for community response, as indicated in Table 7-1 [ISO 1971]. The data in Table 7-1 were derived from responses to noise sources other than wind turbines. Because there has been

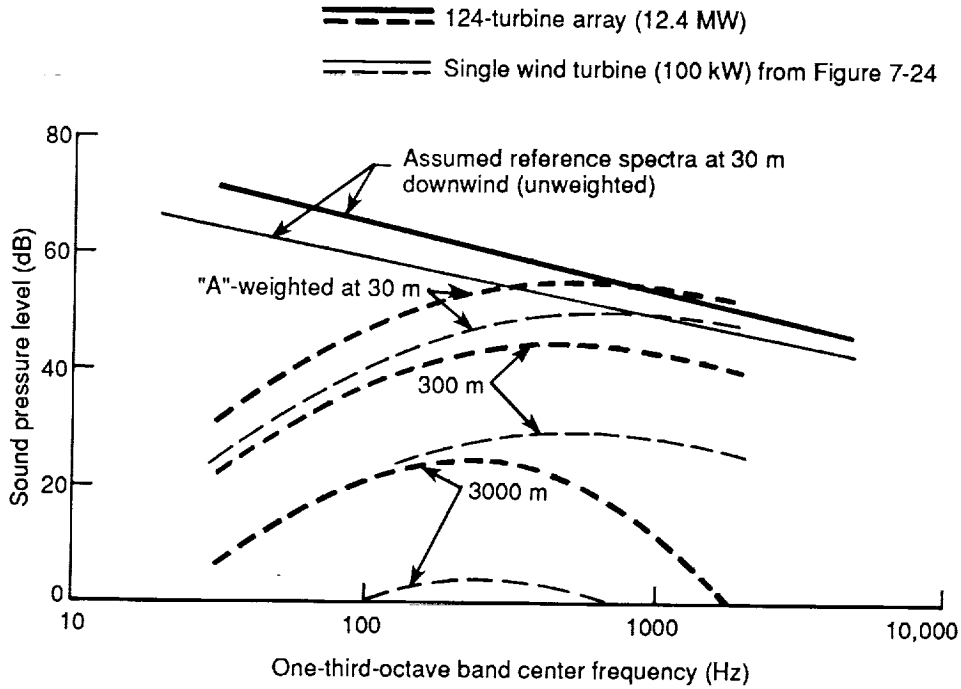

Figure 7-31. Reference and A-weighted noise spectra for the example wind power station and a single wind turbine [Shepherd and Hubbard 1986]

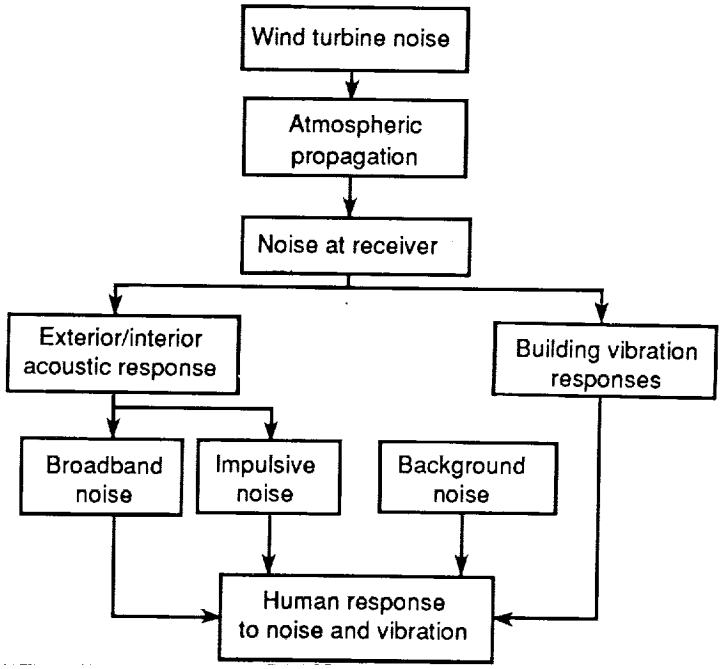

Figure 7-32. Method for evaluating human response to wind turbine noise [Stephens *et al.* 1982]

little experience to date with communities' responses to wind turbines, the applicability of Table 7-1 is tentative. The substantial variations in background noise in terms of time and location are complicating factors.

Perception thresholds for acoustic noise and structural vibrations were derived separately. There are no known threshold criteria for combined effects, except in terms of the quality of the ride in transportation vehicles [Stephens 1979].

Table 7-1. Estimated Community Response to Noise (ISO 1971)

Amount by which Rated Noise Exceeds Threshold Level (dB)	Estimated Community Response	
	Category	Description
0	None	No observed reaction
5	Little	Sporadic complaints
10	Medium	Widespread complaints
15	Strong	Threats of community action
20	Very Strong	Vigorous community action

Perception of Noise Outside Buildings

Evaluating people's responses to wind turbine noise outside buildings involves the physical characteristics of the noise of the machines, the pertinent atmospheric phenomena, and the ambient or outdoor background noise at the receiver's location. Both broadband and narrow-band noise components must be considered if they are present in the noise spectrum.

In Figure 7-33, a one-third-octave band spectrum of broadband wind turbine noise is compared with a one-third-octave band spectrum of typical background noise in a residential neighborhood. In this case, the background noise is the result of noises from numerous distant sources, with no dominant specific source. Wind effects are also absent. Note that the turbine noise levels are generally lower than the background noise levels, except at 1000 Hz, where they are about equal. In the laboratory, humans can just perceive the wind turbine noise when exposed to the spectra of Figure 7-33. High-frequency wind turbine noise is generally not perceived in laboratory tests when the turbine's one-third-octave band levels are below the corresponding levels of background noise (which, in this case, had small temporal fluctuations).

The same general findings apply to the perception of low-frequency impulsive noise. A series of laboratory tests [Stephens *et al.* 1982; Shepherd 1985] were conducted to determine the detection thresholds of impulsive wind turbine noises in the presence of ambient noise with a spectral shape similar to that in Figure 7-33. In contrast to the relatively simple detection model for higher-frequency noises, understanding the perception of low-frequency impulsive noise requires that full account be taken of the blade passage frequency of the wind turbine, the ambient noise spectrum, and the absolute hearing threshold (because the human ear is relatively insensitive to low frequencies).

In addition to laboratory tests with sample spectra, field tests can be used to determine thresholds of perception around wind turbines, including directivity effects. For example, aural (hearing) detectability contours were determined for two large-scale HAWTs surrounded by flat terrain. The results are shown in Figure 7-34.

In Figure 7-34, each data point represents observations of one or two people and defines the distance at which the wind turbine noise is heard intermittently. The two aural curves in the figure are then estimated from these observations and from a limited number of sound pressure measurements. Both curves are foreshortened in the upwind direction

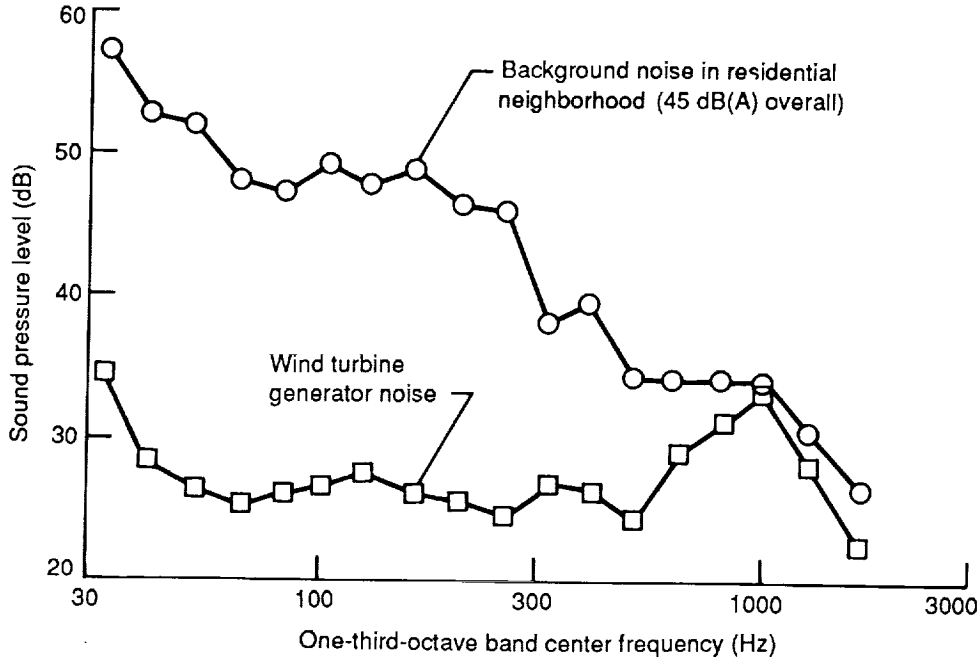

Figure 7-33. Example broadband noise spectrum at the perception threshold in the presence of the given background noise spectrum [Stephens *et al.* 1982]

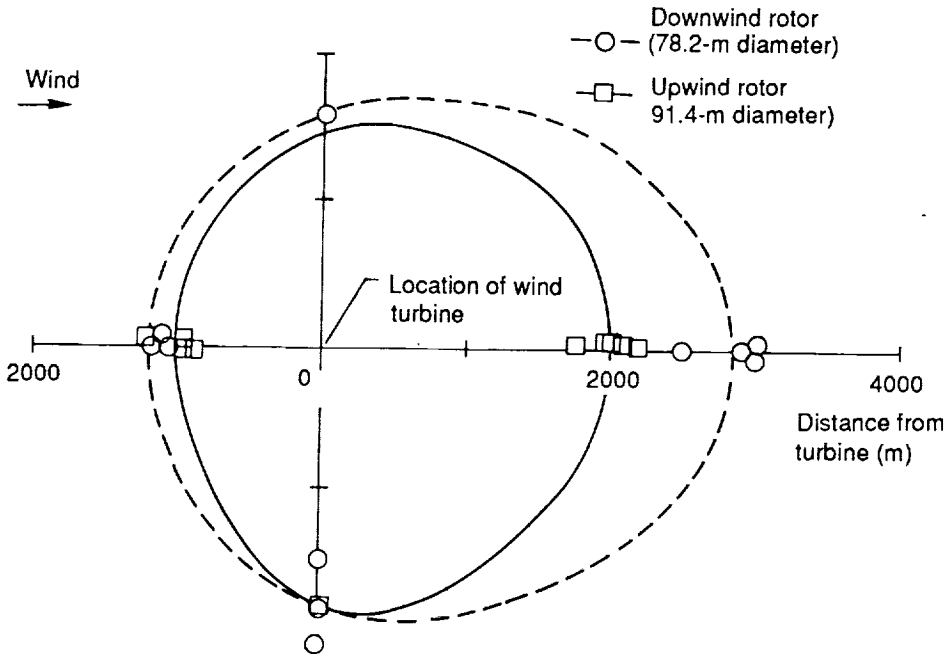

Figure 7-34. Perception thresholds for large-scale HAWTs with downwind and upwind rotors

and elongated in the downwind direction. With one exception, broadband noise was the dominant component perceived for both HAWTs. For the downwind-rotor machine, low-frequency impulses are the dominant component in the downwind direction. This accounts for its longer downwind detection distance as compared with that of the upwind-rotor turbine.

Background Noise

Because background noise is an important factor in determining people's responses to wind turbine noise, it must be carefully accounted for in site measurements. Sources of background noise are the wind itself; its interaction with structures, trees, and vegetation; human activities; and, to a lesser extent, birds and animals. Natural wind noises are particularly important because they can mask wind turbine noise (the broadband spectra of both are similar). Measuring background noise, at the same locations and with the same techniques used for measuring wind turbine noise, is an integral part of assessing receiver response.

Noise Exposure Inside Buildings

People who are exposed to wind turbine noise inside buildings experience a much different acoustic environment than do those outside. The transmitted noise is affected by the mass and stiffness characteristics of the structure, its dynamic responses, and the dimensions and layouts of the rooms. They may actually be more disturbed by the noise inside their homes than they would be outside [Kelley *et al.* 1985]. Indoor background noise is also a significant factor.

Data showing the reduction in outdoor noise provided by typical houses are given in Figure 7-35 as a function of frequency. The hatched area shows experimental results obtained from a number of sources [Stephens *et al.* 1982]. The noise reduction values of the ordinate are the differences between indoor and outdoor levels. The most obvious conclusion here is that noise reductions are larger at higher frequencies. This implies that a spectrum measured inside a house will have relatively less high-frequency content than that measured outside. These data are derived from octave-band measurements but are generally not sensitive to frequency bandwidth.

Very few data are available on outdoor-to-indoor noise reduction at the lowest frequencies (below 50 Hz). In this range, the wavelengths are comparable to the dimensions of the rooms, and there is no longer a diffuse sound field on the inside of the building. Other complicating factors are low-frequency building resonances and air leaks. The inside distribution of sound pressure can be nonuniform because of structure-borne sound, standing wave patterns, and cavity resonances in rooms, closets, and hallways.

Data relating to the noise-induced vibration responses of houses are summarized in Figure 7-36, in which RMS acceleration levels are plotted as a function of external sound pressure level. The trend lines for windows, walls, and floors are averaged from a large number of test measurements on aircraft and helicopter noises, sonic booms, and wind turbine noise.

Gradients and Resonances for Indoor Sound Pressure Levels

Large spatial variations in sound pressure level may occur within a house for uniform external noise excitation. People moving within the house could be sensitive to these variations. Figure 7-37 illustrates the sound-pressure-level gradients in a hallway with various combinations of open and closed doors. Noise was produced by a loudspeaker at a discrete frequency of 21 Hz. This frequency represents the low-frequency noise components from

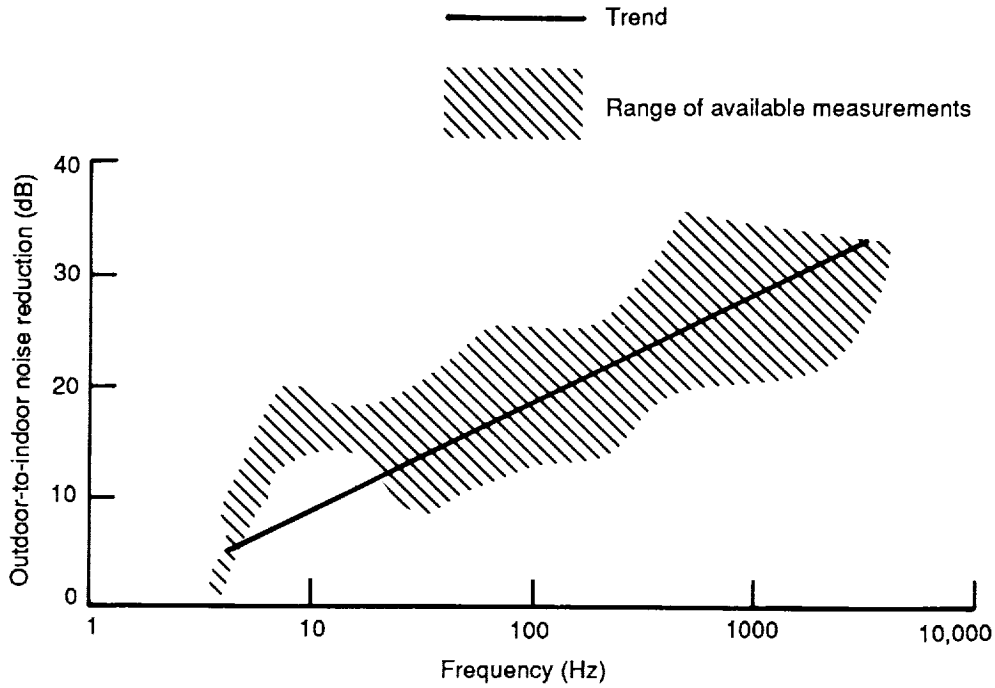

Figure 7-35. Outdoor-to-indoor noise reduction in a typical house with closed windows [Stephens *et al.* 1982]

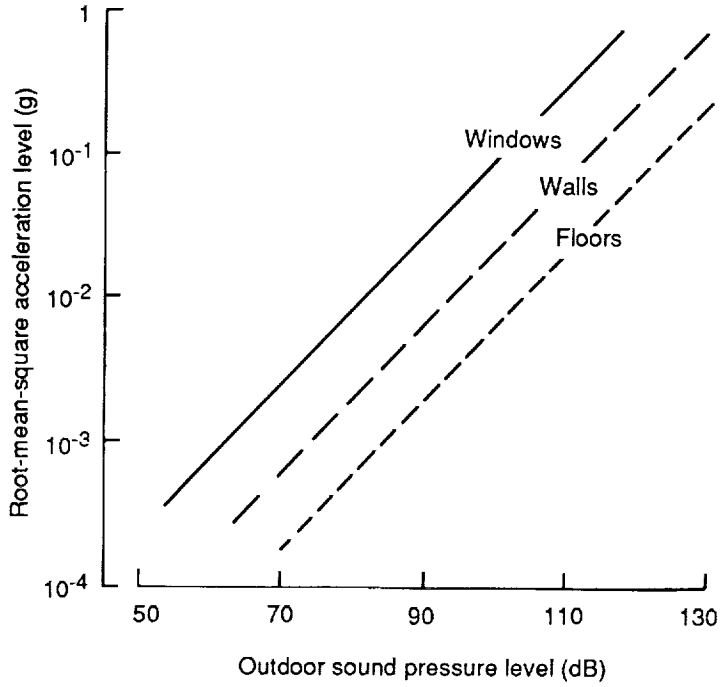

Figure 7-36. The noise-induced acceleration of the typical structural elements of a house, as a function of outdoor sound pressure level [Stephens *et al.* 1982]

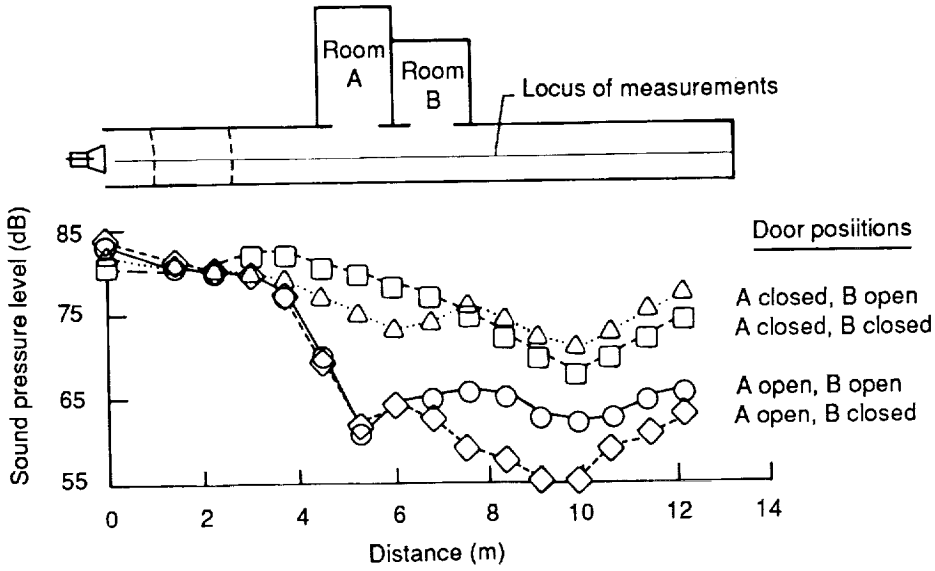

Figure 7-37. Sound-pressure-level gradients in a hallway excited by a pure-tone (21 Hz), constant-power loudspeaker [Hubbard and Shepherd 1986]

wind turbines that would propagate efficiently through buildings. When doors to Rooms A and B are both closed, there is a general decrease in sound pressure level with distance up to the end of the hallway. When doors are open in various combinations, the hallway levels are affected (in some cases, substantially). The changes in level that occur when doors are opened are similar to what might occur for side-branch resonators in a duct.

Because of the way rooms are arranged in houses, it is possible that Helmholtz (cavity) resonances may be excited at certain frequencies, depending on the volumes of the rooms and whether doors are open or closed [Davis 1957; Ingard 1953]. Hubbard and Shepherd [1986] present results of sound-pressure-level surveys conducted inside a room during resonance. For this condition, the inside pressures were everywhere in phase and tended to be a uniform level. This is in contrast to the large gradients observed in the excitation of normal acoustic modes in a room [Knudsen and Harris 1978]. The latter modes are excited at frequencies for which the acoustic half-wavelengths are comparable to or less than the room dimensions, whereas Helmholtz resonance wavelengths are characteristically large compared with the room dimensions. Rooms A and B both exhibit Helmholtz resonance behavior at 21 Hz.

Coupling Noise Fields in Adjacent Rooms

As the sound-pressure-level gradients change in a hallway outside rooms according to whether doors are open and closed (Figure 7-37), so also do the levels inside the rooms. Figure 7-38 illustrates the manner in which these changes occurred for the various test conditions. Variations in sound pressure level are as high as 20 dB for a steady noise input, both inside the rooms and in the hallway (Figure 7-37). This implies that a person might experience a change in levels of this order of magnitude at a particular location, depending on the doors, or as a function of location for a particular door arrangement. During the tests, the highest sound pressure levels of Figure 7-38 could be readily heard; the lowest levels were not audible.

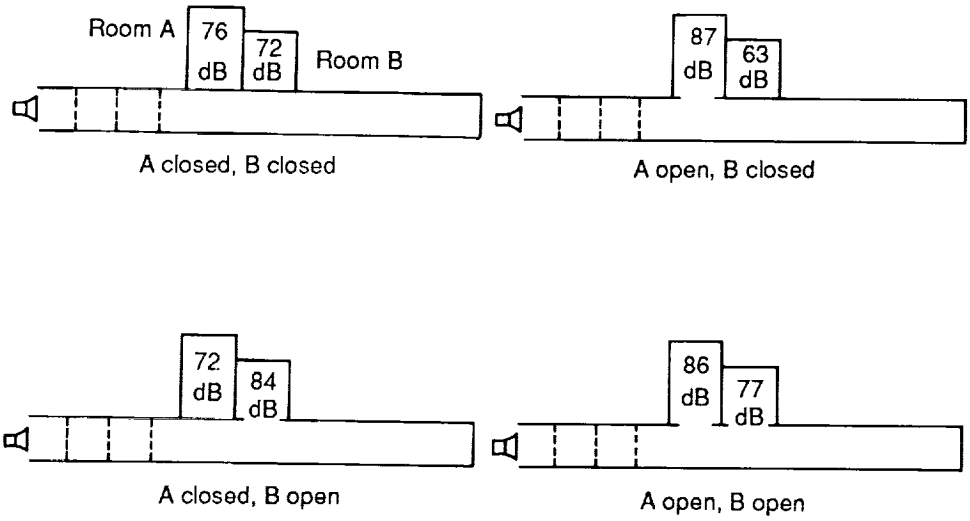

Figure 7-38. Effect of door positions on the maximum sound pressure levels in rooms adjacent to a hallway excited by a loudspeaker (21 Hz) [Hubbard and Shepherd 1986]

Mechanical coupling between adjacent rooms may also excite acoustic resonances, as indicated by data in Hubbard and Shepherd [1986]. One wall of a test room was mechanically excited, and two response peaks were noted. One peak corresponded to the Helmholtz mode of the room, and the other was the first structural mode of the wall. Measured sound-pressure-level gradients were small in both cases.

Perception of Building Vibrations

One of the common ways that a person might sense the noise-induced excitation of a house is through structural vibrations. This mode of observation is particularly significant at low frequencies, below the threshold of normal hearing.

No standards are available for the threshold of perception of vibration by occupants of buildings. Guidelines are available, however, that cover the frequency range from 0.063 to 80 Hz [Hubbard 1982; ISO 1987]. The appropriate perception data are reproduced in Figure 7-39. The hatched region in this figure shows the perception threshold data obtained in a number of independent studies. Different investigators, using different measurement techniques, subjects, and subject orientations, have obtained perception levels extending over a range of about a factor of 10 in vibration amplitude. The composite guidelines of Figure 7-39 are judged to be the best representation of the most sensitive cases from the available data on whole-body vibration perception.

The two cross-hatched regions in Figure 7-39 are from the data of Kelley *et al.* [1985]. These are estimates of levels of vibration perceived in two different houses excited by noise from the MOD-1 wind turbine. The latter data fit within the body of test data on which the composite International Standards Organization guideline is based. Therefore, they generally confirm the applicability of this guideline for structural vibrations induced by wind turbine noise.

Note that, if measured vibration levels are not available, they can be estimated for typical house building elements from Figure 7-36, provided the external noise excitation levels are known.

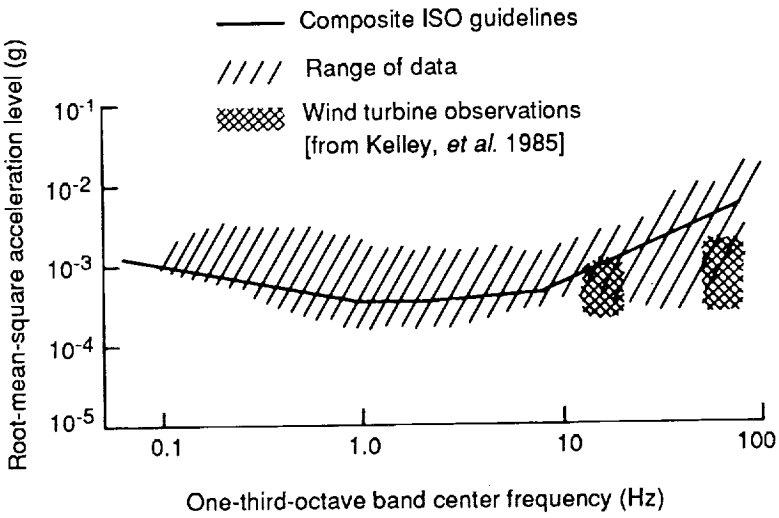

Figure 7-39. Most sensitive threshold of perception of vibratory motion [Stephens *et al.* 1982]

Measuring Wind Turbine Noise

Wind turbine noise is measured to define source characteristics, to provide acoustic information for environmental planning, and to validate compliance with existing ordinances. It is important to use the appropriate equipment and measurement procedures and acquire data under appropriate test conditions. Measuring noise from wind turbine generators is particularly difficult because of the adverse effects of the wind [Andersen and Jakobsen 1983; Jakobsen and Andersen 1983]. As a result, a number of special considerations are involved in selecting measurement locations and equipment and in recording and analyzing data. This section presents some guidelines on each of these subjects.

To make meaningful comparisons of the noise outputs of different wind turbines and evaluations of environmental noise control, it is necessary to have generally accepted standards of measurement. AWEA [1988] and IEA-WECS [1988] contain the results of early work in the wind energy community to develop such standards. Both documents address significant issues in the measurement of wind turbine noise.

To interpret acoustic measurements, it is usually necessary to simultaneously record various nonacoustic quantities. Among these are wind speed and direction, ambient temperature and relative humidity, rotor speed, power output, time of day and date, type of vegetation and terrain, and cloud cover. Atmospheric turbulence (which is often difficult to measure directly) may be inferred from this information.

Measuring Points

Most noise measurements other than those for research purposes are made to characterize the radiated noise of a particular machine. This infers that all data should be obtained far enough from the machine to be in the acoustic far field. For practical applications, the reference distance do should be approximately equal to the total height of a HAWT or, in the case of a VAWT, the total height plus the rotor equatorial radius, as illustrated in Figure 7-40 [IEA-WECS 1988]. The choice of a much greater distance for measurement locations may not be acceptable because of the reduced signal-to-noise ratio and because atmospheric attenuation and refraction effects can complicate the data

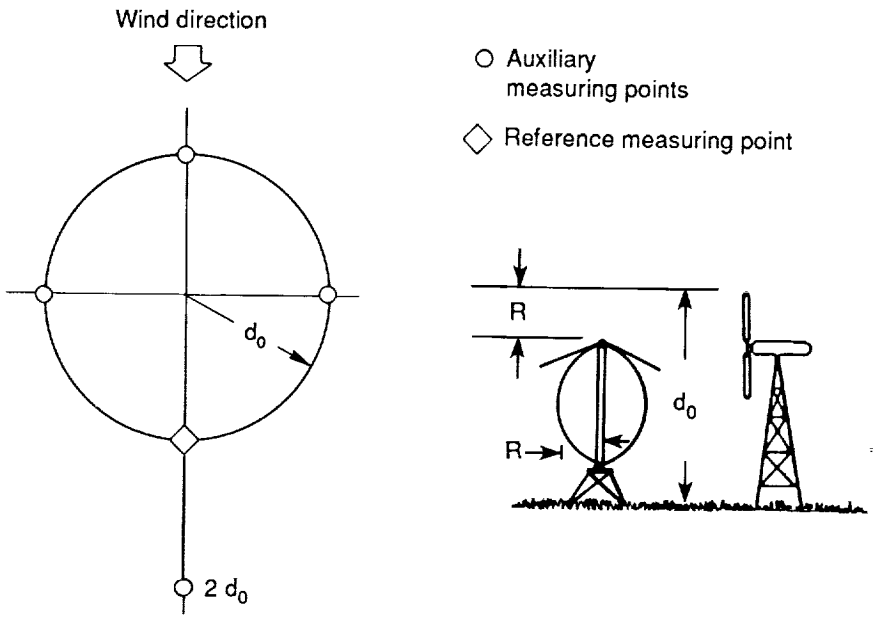

Figure 7-40. Recommended patterns of measuring points for acoustic surveys of wind turbines [IEA-WECS 1988]

interpretation. To ensure the best possible signal-to-noise ratio, the measurement points should be as close to the source as possible without being in the acoustic near-field.

The number of measurement points needed can be determined by inspecting the polar diagrams in Figures 7-6 and 7-7. The aerodynamic noise sources in wind turbines are not highly directional, but the highest levels are usually in the upwind and downwind quadrants. A rather coarse azimuth spacing seems adequate to describe these aerodynamic radiation patterns because they are generally symmetrical about the axis of rotation of the machine. If a particular turbine produces significant mechanical noise, however, its radiation pattern may be asymmetrical and highly directional.

Microphone Positions

An important consideration in laying out a measurement program is defining microphone height above the ground. Placing the microphone at ear level is conceptually attractive because it should record what people hear. The disadvantage of this height is that the data are more difficult to interpret. Figure 7-41 illustrates how the data for sound pressure level may be affected by microphone height, and compares the data to results in free field conditions (i.e. away from all reflecting surfaces). The solid curve represents a calculated spectrum from a point source (such as a gear box) located 20 m above hard ground and received at a microphone position 1.2 m above ground and 40 m from the source. These maximum and minimum points represent interference patterns caused by differences in the distances traveled by the direct sounds and those reflected from the ground surface. Under ideal conditions (with no mean wind or turbulence and perfect ground reflection), the levels vary alternately from 6 dB above free field values to very low values. For an assumed incoherent ring source with a 20-m diameter (which represents the broadband aerodynamic noises) the short-dash curve applies. For a microphone height of 1.2 m, the variation of sound pressure level with frequency from a distributed source is less than that for a point source but it is still significant.

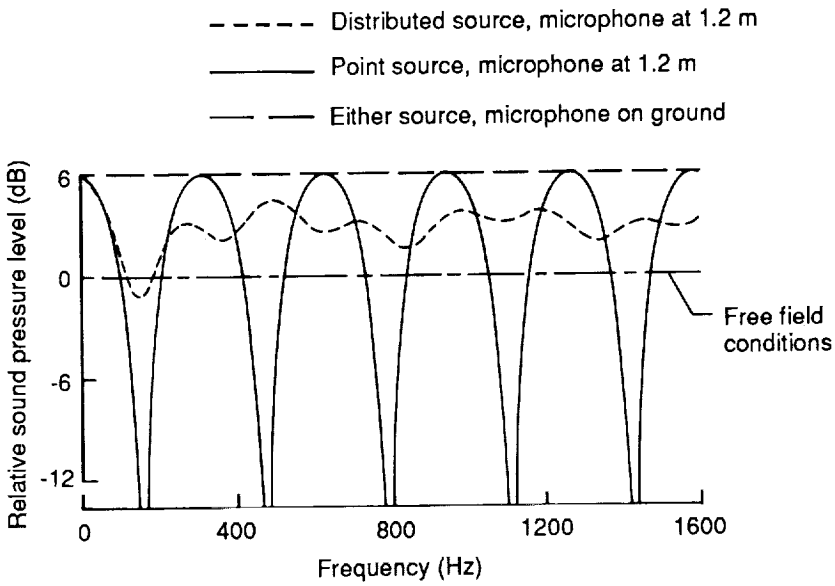

Figure 7-41. Calculated effect of microphone height on the measured noise spectra for point and distributed sources

A measurement at the ground surface, however, gives a constant enhancement above free field values that is 6 dB over the entire frequency range, as indicated by the line of long dashes in Figure 7-41. Thus, it is common practice to place microphones at ground level on a hard, reflecting surface (such as plywood) and then deduct 6 dB from all measured sound pressure levels. When there are very low-frequency components, calculations suggest that microphone placement is not critical. The first dip in the spectra occurs at a frequency well above that associated with low-frequency rotational harmonics, as shown in Figure 7-5.

Acoustic Instrumentation

The requirements for acoustic instrumentation are derived from the type of measurements to be performed and most directly from the frequency range of concern. For the frequency range of 20 to 10,000 Hz, standardized equipment is available for detecting, recording, and analyzing the acoustic signals. A number of different microphones with flat frequency responses are available. Likewise, sound-level meters that meet existing acoustic standards are available for direct readout or for use as signal conditioners before tape recording. Either frequency-modulated or direct-record tape systems may be used.

For cases where the frequency range of measurements must extend below 20 Hz, some special items of equipment may be required. Although standard microphone systems may be used, their frequency response is poor at the lowest frequencies. For increased fidelity, special microphone systems may be required, along with special procedures to minimize wind noise problems. A frequency-modulated tape recorder may also be required, although some direct-record systems may be acceptable if the record speed is slow and the playback speed is fast.

Because wind noise can fill much of the dynamic range of a tape recorder, it may be expedient to use dual-channel recording. In this type of recording, a high-pass filter in one of two tape recorder channels permits the simultaneous recording of low- and high-frequency segments of the same noise signal. The improved signal-to-noise ratio of the high-frequency segment enhances the signal processing.

Windscreen Applications

Measured noise in the presence of wind is contaminated by various types of wind-related noises. These include natural wind noise, or the noise of the wind originating from atmospheric turbulence; microphone noise, caused by the aerodynamic wake of the microphone or microphone windscreen; vegetation noise, caused by the interaction of the wind with nearby vegetation such as trees, bushes, and ground cover; and noise from the aerodynamic wakes of accessories such as a tripod or a nearby structure.

Because of the deleterious effects of the wind, windscreens are recommended to reduce microphone noise for all measurements of wind turbine noise. Commercial windscreens of open-cell polyurethane foam are usually adequate for routine measurements at or near ground level, where wind speeds are relatively low. For measurements above ground, larger, customized windscreens may be necessary [Sutherland, Mantley, and Brown 1987]. It is essential that the acoustic insertion loss of any windscreen be either zero or known as a function of frequency, so that appropriate corrections may be made to the measured data.

Wind noise is a particularly severe problem at the lowest frequencies. The ambient (wind related) noise spectrum increases as frequency decreases, with the result that some low-frequency wind turbine noise components may be submerged in the ambient noise at the microphone location. In such situations, customized windscreens may help reduce the low-frequency wind noise. Some special cross-correlation analysis techniques have also been applied that use measurements from pairs of microphones [Bendat and Piersol 1980].

Little can be done to reduce noise from vegetation, other than to locate microphones away from significant sources. Noise generated by the aerodynamic wakes of accessories such as tripods may be reduced by streamlining these accessories.

Data Analyses

The data analyses required depend on the types of acoustic information required. If A-weighted data are needed, they can be obtained directly from a sound-level meter or from tape recordings and A-weighting filters. Statistical data can also be obtained directly by means of a community noise analyzer or subsequently from tape recordings. Broadband data are routinely produced from one-third-octave band analyses such as that illustrated in Figure 7-8. Narrow-band analyses can be obtained with the aid of a wide range of filter bandwidths, the main requirement being that the bandwidth is small compared to frequency intervals between discrete frequency components.

References

American National Standards Institute (ANSI), 1978, "Method for the Calculation of the Absorption of Sound in the Atmosphere," ANSI SI.26, New York: Acoustical Society of America.

American Wind Energy Association (AWEA), 1988, "Standard Performance Testing of Wind Energy Conversion Systems," Standard AWEA 1.2-1988, Alexandria, Virginia: American Wind Energy Association.

Andersen, B., and J. Jakobsen, Dec. 1983, *Noise Emission from Wind Turbine Generators. A Measurement Method*, Danish Acoustical Institute Technical Report No. 109, Lyngby, Denmark: Danish Academy of Technical Sciences.

Bendat, J. S., and A. G. Piersol, 1980, *Engineering Applications of Correlation and Spectral Analysis*, New York: John Wiley and Sons.

Brooks, T. F., and T. H. Hodgson, June 1980, "Prediction and Comparison of Trailing Edge Noise Using Measured Surface Pressures," Preprint 80-0977, American Institute of Aeronautics and Astronautics.

Brooks, T. F., and M. A. Marcolini, Feb. 1986, "Airfoil Tip Vortex Formation Noise," *AIAA Journal.*, Vol. 24, No. 2.

Daigle, G. A., T. F. W. Embleton, and J. E. Piercy, Mar. 1986, "Propagation of Sound in the Presence of Gradients and Turbulence Near the Ground," *Journal of the Acoustical Society of America*, Vol. 79 No. 3.

Davis, D. D. Jr., 1957, "Acoustical Filters and Mufflers," *Handbook of Noise Control*, Edited by C. M. Harris, New York: McGraw Hill.

George, A. R., 1978, "Helicopter Noise State-of-the-Art," *Journal of Aircraft*, Vol. 15, No. 11, pp. 707-711.

George, A. R., and S. T. Chou, Aug. 1984, "Comparison of Broadband Noise Mechanisms, Analyses, and Experiments on Rotors," *Journal of Aircraft*, Vol. 21.

Glegg, S. A. L., S. M. Baxter, and A. G. Glendinning, 1987, "The Prediction of Broadband Noise for Wind Turbines," *Journal of Sound and Vibration.*, Vol. 118, No. 2, pp. 217-239.

Greene, G. C., Feb. 1981, *Measured and Calculated Characteristics of Wind Turbine Noise*, NASA CP-2185, Cleveland, Ohio: NASA Lewis Research Center.

Greene, G. C., and H. H. Hubbard, May 1980, *Some Effects of Non-Uniform Inflow on the Radiated Noise of a Large Wind Turbine*, Hampton, Virginia: NASA Langley Research Center. **NASA TM-8183.**

Grosveld, F. W., 1985, "Prediction of Broadband Noise from Horizontal Axis Wind Turbines," *AIAA Journal of Propulsion and Power*, Vol. 1, No. 4.

Hawkins, J. A., July 1987, *Application of Ray Theory to Propagation of Low Frequency Noise from Wind Turbines*, NASA CR-178367, Hampton, Virginia: NASA Langley Research Center.

Hubbard, H. H., 1982, "Noise Induced House Vibrations and Human Perception," *Noise Control Engineering Journal*, Vol. 19, No. 2.

Hubbard, H. H., and K. P. Shepherd, Dec. 1982, *Noise Measurements for Single and Multiple Operation of 50 kW Wind Turbine Generators*, NASA CR-166052, Hampton, Virginia: NASA Langley Research Center.

Hubbard, H. H., and K. P. Shepherd, Feb. 1984, *The Effects of Blade Mounted Vortex Generators on the Noise from a MOD-2 Wind Turbine Generator*, NASA CR-172292, Hampton, Virginia: NASA Langley Research Center.

Hubbard, H. H., and K. P. Shepherd, Sept. 1986, *The Helmholtz Resonance Behavior of Single and Multiple Rooms*, NASA CR-178173, Hampton, Virginia: NASA Langley Research Center.

Hubbard, H. H., and K. P. Shepherd, 1988, *Wind Turbine Acoustics Research Bibliography with Selected Annotation*, NASA TM 100528, Hampton, Virginia: NASA Langley Research Center.

IEA-WECS, 1988, "Recommended Practices for Wind Turbine Testing 4. Acoustics Measurement of Noise Emission from Wind Turbines," Submitted to the Executive Committee of The International Energy Agency Programme for Research and Development on Wind Energy Conversion Systems, Second Edition, Bromma, Sweden: Aeroacoustical Research Institute of Sweden.

Ingard, U., Nov. 1953, "On the Theory and Design of Acoustic Resonators," *Journal of the Acoustical Society of America*, Vol. 25, No. 6.

International Standards Organization (ISO), 1971, "Community Response to Noise," ISO Standard R 1996-1971 (E), New York: Acoustical Society of America.

International Standards Organization (ISO), 1987, "Evaluation of Human Exposure to Whole Body Vibration - Part 2: Human Exposure to Continuous and Shock-Induced Vibrations in Buildings (1 Hz to 80 Hz)," Draft ISO Standard 2631-2.2, New York: Acoustical Society of America.

Jakobsen, J., and B. Andersen, Dec. 1983, *Wind Noise Measurements of Wind-Generated Noise from Vegetation and Microphone System*, Danish Acoustical Institute Technical Report No. 108, Lyngby, Denmark: Danish Academy of Technical Sciences.

Kelley, N. D., R. R. Hemphill, and H. E. McKenna, May 1982, "A Comparison of Acoustic Emission Characteristics of Three Large Wind Turbine Designs," *Proceedings of Inter-Noise '82*, New York: Noise Control Foundation.

Kelley, N. D., R. R. Hemphill, and D. L. Sengupta, Oct. 1981, "Television Interference and Acoustic Emissions Associated with the Operation of the Darrieus VAWT," *Proceedings of the 5th Biennial Wind Energy Conference and Workshop*, Vol. I, SERI/CP-635-1340.

Kelley, N. D., H. E. McKenna, R. R. Hemphill, C. L. Etter, R. C. Garrelts, and N. C. Linn, Feb. 1985, *Acoustic Noise Associated with the MOD-1 Wind Turbine: Its Source, Impact and Control*, SERI TR-635-1166, Golden, Colorado: Solar Energy Research Institute.

Kelley, N. D., H. E. McKenna, E. W. Jacobs, R. R. Hemphill, and N. J. Birkenheuer, Oct. 1987, *The MOD-2 Wind Turbine: Aeroacoustical Noise Sources, Emissions, and Potential Impact*, SERI/TR-217-3036, Golden, Colorado: Solar Energy Research Institute.

Knudsen, V. O., and C. M. Harris, 1978, *Acoustical Designing in Architecture*, New York: American Institute of Physics.

Lowson, M. V., Nov. 1970, "Theoretical Analysis of Compressor Noise," *Journal of the Acoustical Society of America*, Vol. 47, No. 1 (Part 2).

Lunggren, S., 1984, *A Preliminary Assessment of Environmental Noise from Large WECS, Based on Experiences from Swedish Prototypes*, FFA TN 1984-48, Stockholm, Sweden: Aeronautical Research Institute of Sweden.

Martinez, R., S. E. Widnall, and W. L. Harris, 1982, *Prediction of Low Frequency Sound from the MOD-1 Wind Turbine*, SERI TR-635-1247, Golden, Colorado: Solar Energy Research Institute.

Meijer, S. and I. Lindblad, 1983, *A Description of Two Methods for Calculation of Low Frequency Wind Turbine Noise, Including Applications for the Swedish Prototype WECS Maglarp*, FFA TN 1983-31, Stockholm, Sweden: Aeronautical Research Institute of Sweden.

Pearsons, K. S., and R. L. Bennett, Apr. 1974, *Handbook of Noise Ratings*, NASA CR-2376, Hampton, Virginia: NASA Langley Research Center.

Piercy, J. E., and T. F. W. Embleton, 1979, "Sound Propagation in the Open Air," *Handbook of Noise Control 2nd Edition*, edited by C. M. Harris, New York: McGraw Hill.

Piercy, J. E., T. F. W. Embleton, and L. C. Sutherland, June 1977, "Review of Noise Propagation in the Atmosphere," *Journal of the Acoustical Society of America*, Vol. 61, No. 6.

SAE, 1966, "Method for Calculating the Attenuation of Aircraft Ground to Ground Noise Propagation During Takeoff and Landing," SAE Aerospace Information Report AIR 923, Warrendale, Pennsylvania: Society of Automotive Engineers.

Schlinker, R. H. and R. K. Amiet, Nov. 1981, *Helicopter Rotor Trailing Edge Noise*, NASA CR-3470, Hampton, Virginia: NASA Langley Research Center.

Sears, W. R., 1941, "Some Aspects of Non-Stationary Airfoil Theory and Its Practical Application," *Journal of Aerospace Sciences*, Vol. 8, No. 3.

Shepherd, K. P., Jan. 1985, *Detection of Low Frequency Impulsive Noise from Large Wind Turbine Generators*, NASA CR-172511, Hampton, Virginia: NASA Langley Research Center.

Shepherd, K. P., and H. H. Hubbard, July 1981, *Sound Measurements and Observations of the MOD-OA Wind Turbine Generator*, NASA CR-165752, Hampton, Virginia: NASA Langley Research Center.

Shepherd, K. P., and H. H. Hubbard, May 1983, *Measurements and Observations of Noise from a 4.2 Megawatt (WTS-4) Wind Turbine Generator*, NASA CR-166124, Hampton, Virginia: NASA Langley Research Center.

Shepherd, K. P., and H. H. Hubbard, Aug. 1984, *Acoustics of the MOD-0/5A Wind Turbine Rotor with Two Different Ailerons*, NASA CR-172427, Hampton, Virginia: NASA Langley Research Center.

Shepherd, K. P., and H. H. Hubbard, Mar. 1985, *Sound Propagation Studies for a Large Horizontal Axis Wind Turbine*, NASA CR-172564, Hampton, Virginia: NASA Langley Research Center.

Shepherd, K. P., and H. H. Hubbard, Apr. 1986, *Prediction of Far Field Noise from Wind Energy Farms*, NASA CR-177956, Hampton, Virginia: NASA Langley Research Center.

Shepherd, K. P., W. L. Willshire, Jr., and H. H. Hubbard, 1988, *Comparisons of Measured and Calculated Sound Pressure Levels around a Large Horizontal Axis Wind Turbine Generator*, NASA TM 100654, Hampton, Virginia: NASA Langley Research Center.

Stephens, D. G., 1979, "Developments in Ride Quality Criteria," *Noise Control Engineering Journal*. Vol. 12, No. 1.

Stephens, D. G., K. P. Shepherd, H. H. Hubbard, and F. W. Grosveld, Mar. 1982, *Guide to the Evaluation of Human Exposure to Noise from Large Wind Turbines*, NASA M-83288, Hampton, Virginia: NASA Langley Research Center.

Sutherland, L. C., R. Mantey, and R. Brown, Sept. 1987, *Environmental and Cumulative Impact of Noise from Major Wind Turbine Generator Developments in Alameda and Riverside Counties—Literature Review and Measurement Procedure Development*, WR87-8, El Segundo, California: Wyle Laboratories.

Thomson, D. W., 1982, *Analytical Studies and Field Measurements of Infrasound Propagation at Howard's Knob, North Carolina*, SERI/TR-635-1292, Golden, Colorado: Solar Energy Research Institute.

Thomson, D. W., May 1982, "Noise Propagation in the Earth's Surface and Planetary Boundary Layers," *Proceedings of Internoise-82*, New York: Noise Control Foundation.

Viterna, L. A., Feb. 1981, *The NASA-LeRC Wind Turbine Sound Prediction Code*, NASA CP-2185, Cleveland, Ohio: NASA Lewis Research Center.

Wehrey, M. C., T. H. Heath, R. J. Yinger, and S. F. Handschin, Mar. 1987, *Testing and Evaluation of a 500-kW Vertical Axis Wind Turbine*, AP-5044, Palo Alto, California: Electric Power Research Institute.

Willshire, W. L. Jr., and W. E. Zorumski, June 1987, "Low Frequency Acoustic Propagation in High Winds," *Proceedings of Noise-Con 87*, New York: Noise Control Foundation.

NASA
National Aeronautics and Space Administration

Report Documentation Page

1. Report No.	2. Government Accession No.	3. Recipient's Catalog No.
NASA TP-3057 DOE/NASA/20320-77		

4. Title and Subtitle	5. Report Date
Wind Turbine Acoustics	December 1990
	6. Performing Organization Code

7. Author(s)	8. Performing Organization Report No.
Harvey H. Hubbard and Kevin P. Shepherd	E-5663
	10. Work Unit No. 776-33-41

9. Performing Organization Name and Address	11. Contract or Grant No.
National Aeronautics and Space Administration Langley Research Center Hampton, VA 23665-5225	
	13. Type of Report and Period Covered: Technical Paper

12. Sponsoring Agency Name and Address	14. Sponsoring Agency Code
U.S. Department of Energy Office of Solar Electric Technologies Washington, D.C. 20545	

15. Supplementary Notes

Prepared under Interagency Agreement DE-AI01-76ET-20320. The text of this report is planned to appear as a chapter in a forthcoming book entitled *Wind Turbine Technology*. This is a joint project of the U.S. Department of Energy and the American Society of Mechanical Engineers, in which the NASA Lewis Research Center is responsible for technical editing and management. Production of the final text is under the sponsorship and direction of DOE's Solar Technical Information Programs Office. Book publication will be by the ASME.

16. Abstract

Available information on the physical characteristics of the noise generated by wind turbines is summarized, with example sound pressure time histories, narrow- and broadband frequency spectra, and noise radiation patterns. Reviewed are noise measurement standards, analysis technology, and a method of characterizing wind turbine noise. Prediction methods are given for both low-frequency rotational harmonics and broadband noise components. Also included are atmospheric propagation data showing the effects of distance and refraction by wind shear. Human perception thresholds, based on laboratory and field tests, are given. Building vibration analysis methods are summarized. The bibliography of this report lists technical publications on all aspects of wind turbine acoustics.

17. Key Words (Suggested by Author(s))	18. Distribution Statement
Wind energy; Wind turbine; Acoustic noise; Noise testing; Noise generation; Noise propagation; Environmental impact; Sound pressure levels	Unclassified – Unlimited Subject Category 71 DOE UC-261

19. Security Classif. (of this report)	20. Security Classif. (of this page)	21. No. of pages	22. Price*
Unclassified	Unclassified	50	A03

*For sale by the National Technical Information Service, Springfield, Virginia 22161